Design of a radial inflow microturbine for a combined heat and power generation unit

Salvador María Beltrán Martínez

LUND
UNIVERSITY

Department of Energy Sciences

MSc Thesis TFRT-LUTMDN/TMHP-21/5474-SE
ISSN 0282–1990

Department of Energy Sciences
Lund University
Box 118
SE-221 00 LUND
Sweden

Printed in Sweden by Media-Tryck.
Lund 2021

Abstract

Microturbines are part of a rapidly growing industry which is at a critical point of development. Their flexibility and ease of coupling make them particularly interesting when searching for efficient energy production solutions in all types of industries.

This Master Thesis aims at the design of a radial-inflow microturbine that is part of a combined heat and power generation unit intended for domestic use. The project belongs to Compower AB, a pioneer Swedish clean Tech company that is located in Lund, Sweden.

In order to identify the important factors before performing the design, an analysis of the non-dimensional groups and the most important parameters for radial turbines are carried out. Afterwards, the microturbine design is performed with the software TurbAero. The main turbine elements such as the volute, the nozzle vanes, the impeller blades and the diffuser are designed. In a radial turbine, the most important components are the nozzle vanes and the impeller blades, what means that, in these cases, the design is performed in more detail. Based on the working conditions provided by the company, a detailed design of various components of the turbine is performed.

This thesis work provides a general overview over the structure and design of radial microturbine for combined heat and power units. It also gives a more efficient design over the existing design. The outcome of which is expected to be tested and commercializaed in the near future.

Acknowledgements

This master thesis marks the end of my university studies in Industrial Engineering and the beginning of my professional life as an engineer. It has been carried out at Compower AB in Lund, Sweden and at the Department of Energy Sciences at the Faculty of Engineering, Lund University.

Firstly, I would like to show my deepest appreciation to my supervisors Narmin Hushmandi and Magnus Genrup from the Department of Energy Sciences for their time and their explanations. They have introduced me on the interesting field of turbomachinery and have helped me to understand all the questions I had along the way.

I would like to thank Mikael Swanteson from Compower AB for having welcomed me to his company, for having explained to me how the project works and for having given me advice when making decisions.

I would like to thank my group of thesis friends Baldo, Amparo, Pepe, Iván and Eric for having walked with me along this learning journey.

Finally, I would like to thank Clara and my family who have been supporting me throughout this important stage of my life.

Nomenclature

α	Flow angle
β	Blade angle
$\dot{m}$	Mass flow rate
γ	Ratio of specific heats
μ	Viscosity
ω	Angular velocity
ϕ	Flow coefficient
ψ	Head coefficient and stage loading coefficient
ρ	Density
θ	Blade camber angle
A	Area
a	Distance to maximum camber in the blade
C	Absolute velocity
c	Chord of the blade
c_m	Meridional velocity in the turbine
C_P	Specific heat at constant pressure
C_V	Specific heat at constant volume
D	Diameter
E	Internal energy

F	Force
H	Head
h	Specific enthalpy
I	Rothalpy
K_M	Correction factor for Mach number effects
K_p	Correction factor for compressibility effects
K_{inc}	Correction factor for off-design incidence effects
K_{RE}	Correction factor for Reynolds number effects
M	Mach number and moment
N	Rotation speed (rpm)
N_N	Number of nozzle blades
N_R	Number of rotor blades
o	Throat
P	Power
p	Pressure
Q	Volume flow rate and heat energy
R	Specific gas constant
r	Radius
R_c	Suction surface radius of curvature at the blade trailing edge
s	Blade pitch
T	Temperature
t	Thickness and time
U	Blade speed
u	Tangential velocity
W	Relative velocity and mechanical energy
Y_p	Profile loss coefficient

Y_{p1}	Nozzle profile loss coefficient
Y_{p2}	Impulse profile loss coefficient
Y_{TE}	Trailing edge loss coefficient
z	Axial and heigh coordinate

Contents

List of Figures

List of Tables

1

Introduction

In this chapter a preliminary overview of the turbines, and specifically the microturbines is given. It is important to know the type of machine we are working with and how it works. This will help us to understand the working principles of the fluid as well as the most important parameters to consider when designing it. We will also talk about the facts that make microturbines attractive and that motivate this work.

1.1 Background

Turbines range from a few kW micro gas turbine to a few hundred MW instrial gas turbine. They are rotating machinery. A fluid passes through the blades at high velocity, and they receive the kinetic energy from it. So, the fluid moves and expands and then it interacts with the rotor blades making them to move, so we have energy transfer in the turbine.

The turbine is a rotatory machine that converts the kinetic energy of the fluid into rotating shaft energy. The main elements of the turbine are the stator or nozzle and the rotor or impeller. The first one is the fixed part, and it is also called guide vanes in hydro turbines. Its function is to accelerate and direct the fluid to the rotor. The second one is formed by a certain number of blades and is the moving part. It is attached to the shaft where also the generator is attached and that generates electricity.

Nowadays, the turbine is more efficient motor compared to internal combustion engines and some electrical engines. We can find it in different types, such as gas turbines, steam turbines, hydraulic turbines, turbochargers, wind turbines, depending on the application and the state of the fluid. Note that the fluid can be compressible and incompressible. And the perfect gas assumption can be applied with good accuracy for many gas turbine fluids.

The microturbines are the smallest size turbines. They usually have high rotational speeds since they normally work at more than 90000 rpm. Microturbines are considered to give a maximum output power of 200 kW approximately. Also, it is important to note that this type of turbine provides much larger power density in a

single stage compared to the other types. Sometimes, units from 200 kW to 500 kW may be called miniturbines.

Microturbines normally produce either heat or electric power. They have a shaft where the rotor is attached, as well as the compressor and the electric generator. Apart from the stator and the rotor, they are usually formed by the compressor, the combustor, the generator, and the recuperator. The recuperator operates by recovering the energy of the exhaust gases and preheating the compressed inlet air to increase the efficiency of the turbine.

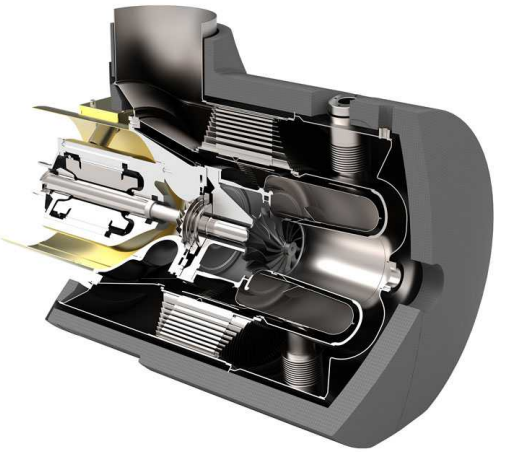

Figure 1.1: Capstone microturbine. Model C65. Output power: 65 kW. Weight: 758 kg [1].

If we compare microturbines to the other traditional types of turbines, we can say that they are more compact since they do not have many moving parts, they are lightweighted and cost-effective. They have minimal emissions and fuel wastage too. Thanks to these advantageous properties they have a huge number of applications and among them we find combined cooling, heating and power (CCHP), microgrid systems and combined power and heat (CHP). In this thesis work, a radial microturbine suitable for a combined heat and power unit (CHP) will be designed and analyzed.

1.2 Motivation

As we have seen, microturbines have a big number of favourable properties. One of them, as we have previously mentioned is that they are compact since they have

a small number of moving parts. This makes them less noisy systems than reciprocating engines. Also, since the main moving part is the impeller, and its only movement is the rotation we can affirm that we do not find excessive vibrations. These two properties together with the small size of the microturbines make them a very suitable option for domestic houses. They can be located on sites with space limitations. The microturbine that is going to be designed in this project is destined to this application.

It is important to know that these domestic units are still relatively expensive but large-scale mass production could realize significant economies of scale. On the other hand, due also to fewer moving parts, it is expected that microturbines do not need frequent technical reviews as the reciprocating engine technologies do. Most manufacturers target maintenance intervals up to 8000 hours that can mean once in a year.

In terms of fuel, microturbines are flexible since they can use a big variety of fuels to run the combustor, that will heat up the air before coming into the expansion phase in the rotor. They can use gas fuels like natural gas or liquid fuels like gasoline or kerosene. In previous microturbine prototypes of Compower AB, biofuel with a high-power density has been used among others.

The installation of a microturbine always means sustainability for these reasons:

- With the recuperator, the microturbine has a higher efficiency compared to models without recuperator.
- Reduces the infrastructure upgrades.
- Minimizes the site disturbance, has a small footprint of CO_2.
- Produces the lowest emission of any noncatalyzed fossil fuel combustion system.

Therefore, as it has been explained, microturbines have a great advantatge over other types of turbine even over many other types of engines. They are a great choice in the economical aspect, as well as in the technical and environmental aspect. This makes them an interesting choice to research, develop and install to several applications.

1.3 The radial microturbines

Now we are going to see what is so special in radial turbines and what makes them different from axial turbomachines. A radial turbine stage is different from an axial stage by having the fluid undergoing a significant radius change in passing through the rotor. Whereas in an axial turbine the fluid enters and leaves in a predominantly axial direction with little or no change in radius, in a radial inflow turbine the fluid enters in the radial inward direction, is turned in the meridional (or axial-radial) plane, and leaves in the axial direction [2].

The flow field

When the fluid enters the rotor we have to focus on the behaviour of the flow field. In the design point of a turbine, the flow comes into the rotor with maximum absolute velocity but with a low relative velocity. This will increase when crossing the rotor blades. When the flow turns in the tangential plane, it creates a pressure gradient in the stage. And this pressure field causes the induced incidence that is characterized by the incidence angle in the leading edge.

It is really useful to look at the flow visualizations of Baines [2] since they are very helpful to understand the flow entering the impeller. They are shown in Fig. 1.2. They are an approximation to the behaviour of the fluid in the current radial turbines since they are part of a experiment that was performed with a low-speed water flow.

As it can be seen, the three cases in the experiment show a movement of the flow from the suction to the pressure surface. The cause of this is the fact that the relative flow vectors move always from the low to the high pressure side in the direction of rotation.

When analysing and designing aerodynamics in turbomachinery it is fundamental to make predictions about the flow behaviour through the cascades of blades. It is a really three dimensional flow problem and the result can be very complex. But, there is also another simpler option to understand the basic flow process. It is the two dimensional blade to blade flow problem

Two dimensional analysis can provide us with an evaluation of the viscousity effects. However, this approach makes doubts in the reliability of this analysis when we look at the flow behaviour in the boundary layer since 3D effects in the flow are ignored.

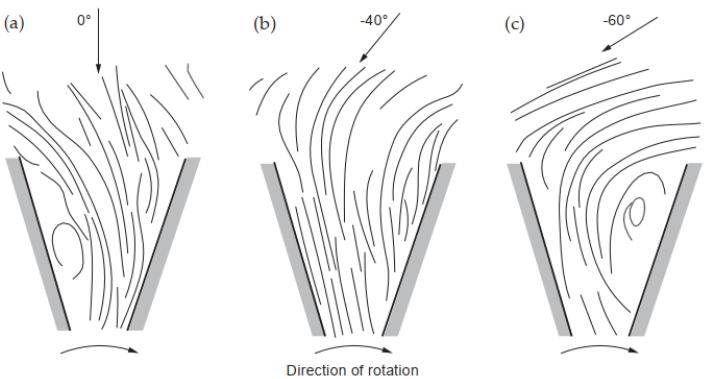

Figure 1.2: Inlet flow pattern for three different incidence angles of an impeller [2].

As it can be seen in the Fig. 1.2, the most uniform flow distribution is the one

of the case (b), where the inlet incidence flow angle is 40º opposite to the direction of rotation. The case (a) is a radial inlet and shows how the flow is separated from the edge of the suction surface and a strong turbulence is created. Finally, in the case (c), where we have the most negative incidence angle something similar to the case (a) happens. The flow is separated from the surface and there are also recirculations. But here, instead of having it in the suction surface, we have it in the pressure surface. In most cases it is not possible to measure the value of the incidence angle directly in the rotor inlet, so it can be deduced from the values of the turbine performance.

Components analysis

Now, the geometry and function of the components involved in a radial turbine stage will be briefly explained. The components are described in the same order as the flow passes through them. It can be useful to follow the explanation by looking at Fig. 1.3.

In radial turbines, the stator plays an essential role. It is the swirl generating component. In most of radial turbines a ring of nozzle vanes is used as a stator to accelerate the fluid and direct it in a right angle to the entry of the rotor. So, the nozzle vanes must be able to accept an incoming radial flow at the inlet and eject it in an almost tangential direction to the rotor.

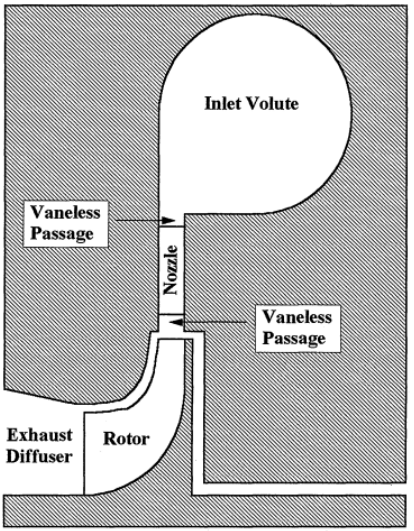

Figure 1.3: Meridional cross section of a half of a radial turbine stage [3].

Sometimes when it is necessary to save space, it is possible to dispense with the stator as long as we have a volute to perform the same function, since it is

capable of achieving the correct inlet conditions to the rotor. This is the case of small turbochargers. But if we want to operate at higher expansion ratios or we want to have a high specific work, we will have a greater swirl at the rotor inlet, so the nozzle vanes will be necessary. In this project, the microturbine will have both the nozzle vanes and the volute.

In Fig. 1.4 the cross section of the inlet volute geometry can be seen in more detail. The flow process is represented in three different stations. Station 1 represents the flow inside volute, but has not yet started to leave into the nozzle row. Once we get past station 1, the flow starts to leave the volute through the exit area. As we see in station 1, the passage area and the mean radius are specified. The same happens at station 2, where half of the flow has left from the volute. And finally we have the station 3 that represents the annular passage at the volute outlet.

Note that this is the first element in the single stage of a microturbine, so the inlet total conditions must be known. Then knowing these, we can have the conditions at station 1 by performing a mass balance between two points. Then, from the conditions of station 1 and assuming no losses and using half of the inlet mass flow we can get the conditions at station 2. Finally, to get the conditions of station 3 we must perform another mass balance using the inlet mass flow and the correspondent tangential velocity. In the following figure a general description is shown.

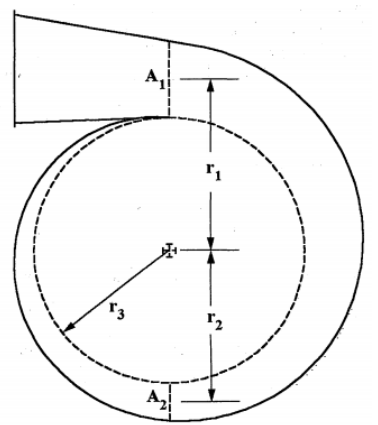

Figure 1.4: Inlet volute geometry [3].

Once the flow exits the volute passage, it enters the stator. The stator or nozzle row in radial turbines is a simple passage of constant width in radial direction. The fact is that in general more specifications about these nozzles are given since the geometry is specified by 3 stations: the inlet, the midpassage throat and the outlet.

To know these stations some parameters of them must be known. These are some of the key geometrical parameters that are shown in the Fig. 1.5: Camber

angle β, blade thickness t_b, throat blade-to-blade width o and radius r. There are other parameters that use to be known that are not shown such as the passage width b or the number of blades N.

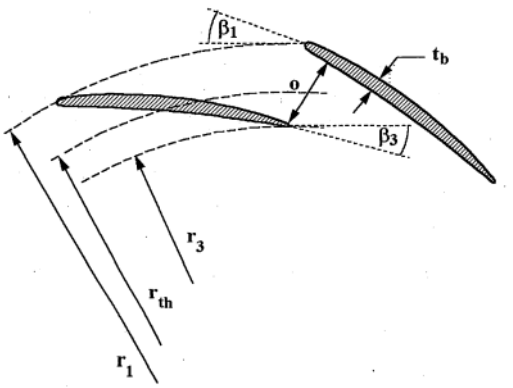

Figure 1.5: Nozzle row geometry, inlet and outlet flow angles together with radial position of different cross sections are specified [3].

After the fluid has passed through the nozzle row, it enters the rotor. The rotor is the most complex element in radial inflow turbines. It is the one with more design possibilities. There the fluid is turned 90º from radial to axial direction are producing flow profile gradients due to the hub-to-shroud curvature. Incidence, blade clearance, passage friction and profile losses are some of the main causes of the internal losses in the impeller. In a similar way to the previous components the geometry passage of the rotor can be defined in three different stations: the inlet, the midpassage and the outlet.

The hub and the shroud are the limit parts when working in the rotor geometry. The hub is the lower diameter part, this is where the root of the blades is attached, whereas the shroud is the outer diameter part, this is the tip or the outermost part of the blade. Impellers can have their blades attached together by a circular ring, the shroud. But more commonly in radial inflow turbines, blades are unshrouded, so they are standing free with a small clearance to the casing and only attached in the hub. In Fig. 1.6, the rotor geometry can be appreciated.

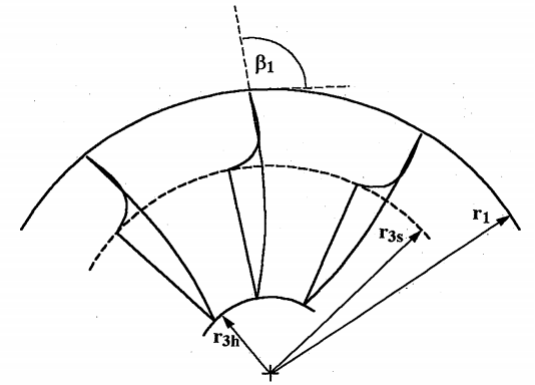

Figure 1.6: Front view of impeller geometry [3].

1.4 State of the art

In this section the current knowledge and experience about the design of microturbines are going to be explained. Since microturbines are getting more and more sophisticated every day, and they are being implemented to a lot of applications this section is a fundamental piece of this work. Through it, an overview of the current status of the development of this technology field is given. Therefore, a description of the knowledge about the studied subject through the analysis of similar or related published work in open literature is carried out.

Many recent studies on the design of nozzle vanes for radial-inflow turbines have been performed. Some of them are related to the outlet flow angle of the vanes and others to the efficiency. Experience has demonstrated to many researchers that the nozzle vanes that have a small outlet angle usually have lower efficiency values.

Fershalov, et. al. [4] presented a new design of the nozzle vanes. They had a rectangular cross section. Fixing the other parameters in the best possible way to this new design of the vanes, it was possible to obtain higher efficiencies for outlet angles from 5º to 9º. Figure 1.7 shows the rectangular nozzle vanes performed in their experiment.

It is important to note that before this experiment, they performed another study and found out that there were different limit values for the outlet angle of the nozzle vanes. Some researchers concluded that an outlet angle of 12º or lower was unacceptable, while others said that the values of the outlet angle could be as low as 9º. That was due to the fact that the smaller the nozzle outlet angle, the greater the kinetic losses.

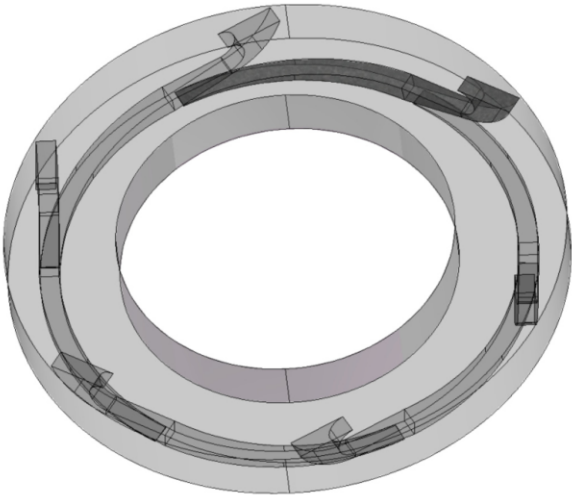

Figure 1.7: Three dimensional geometry of the nozzle vanes with rectangular section [4].

On the other hand, Ibragimov [5] performed an study and presented his experimetal data of microturbine stages with small outlet angles of nozzle. His result is shown in Fig. 1.8 where π represents the pressure difference for a stage; α_{1k} is the outlet angle of the nozzle vanes; and the vertical axis is referred to the efficiency factor.

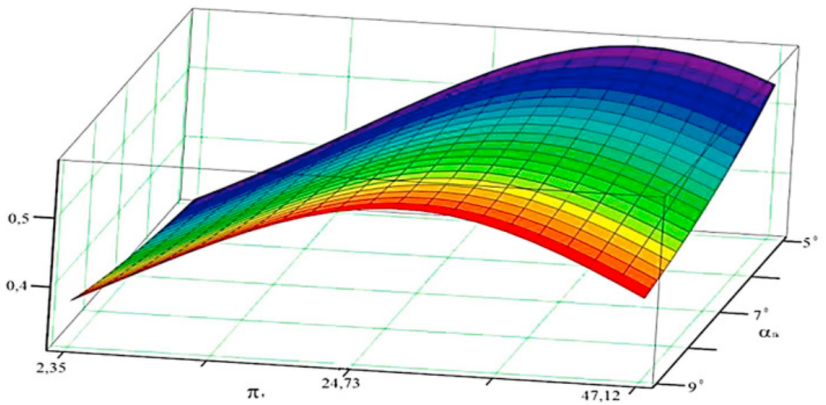

Figure 1.8: Three dimensional chart of outlet angle of nozzle vanes, efficiency factor and pressure difference [5].

In the figure above, it can be seen that for small values of π and high values of α_{1k}, the efficiency factor tends to grow. Then, for large values of π with the increase of α_{1k}, the efficiency factor decreases. Therefore, the authors concluded that the experimental results confirm that getting high efficiency levels for small outlet angles is possible.

There are also several recent studies and experiments about turbine profiling methods that can be applied to microturbines. For instance, Fershalov [6] presented a new principle for designing microturbine stages based on the partial integration of cylindrical visors in the rotor. In the experiment, an axial microturbine with a single stage was used as a model, and it was compared to a reference turbine. The results showed that the tested turbine gave a better efficiency than the reference one. Therefore the authors concluded that the microturbine design using this principle was highly efficient. In addition, the authors state that this profiling method can be used for turbines with other sizes.

Finally, the studies outlined above are just a few examples of the research work that is being carried out about the microturbines. This serves as a motivation for the design of the microturbine of the this work.

Product development

In this section the methods of development in the world of microturbines are going to be explained. The idea is to get a general overview about the current situation of the research in microturbines through two examples. The first one is going to be related to the emission or ecological part and on the other hand, the second one is going to be related to the connection and the adaptability of microturbine systems.

Hydrogen as fuel

Nowadays it is getting more and more common that the microturbines companies are looking for having a cleaner and greener image about themselves. And not only because of the image of the companies but because many clients look for the most clean and least CO_2 emission installations. That's why the most clean tech pioneer companies have started to use hydrogen as the main fuel in microturbines.

The long term prospects for companies that are always working on the reduction of emissions are quite good. The development of hydrogen-blending technologies is directly related to the sales growth. Currently, companies are trying to increase the hydrogen percentage of the fuel. A normal case could be to have a hydrogen content between 10% and 30% in the fuel.

Researchers at Argonne National Laboratory from Chicago are running hydrogen injector in simulations to test a 70% hydrogen and 30% percent natural gas mix. From this tests, a good feedback of the injector performance will be obtained. This process of getting the perfect mixture is quite similar to the traditional combustion engine technology. The main issue here is that it is necessary to work with

a smaller hydrogen molecule. This makes the fuel much more volatile, which is a hard challenge [7].

The hydrogen demand has increased in a fast way in the last two years. Hydrogen is a clean fuel source and when it is used in a fuel cell, it produces only water. Moreover, hydrogen can be obtained from water thanks to electrolysis. But now, since the cost of electrolyzers is quite high, the cost of green hydrogen is also high.

Finally, this is getting one of the most important developing ways in microturbines and even more since the market is supporting the use of hydrogen as main fuel.

Connection to microgrids

Climate change and sustainable development, have caused an uprising trend of development efforts either on both local and international scale. The United Nation General Assembly laid out one of the most challenging sustainable goals to “ensure access to affordable, reliable, sustainable modern energy for all" [8].

Then it is getting more and more necessary the development of renewable-integrated micro energy systems. The reliability and the flexibility on capacity are requirements that must be met by these systems.

Microturbines are one of the most efficient and multifaceted energy technologies and they can easily be integrated with renewable sources in several ways. Considering their versatility, they can be either connected in isolated as well as distributed generation systems.

On the other hand, microgrids are interconnected loads, generators and storage that act as a single controllable system to the grid. Since the interest in integrating renewable energy generators is increasing and that microgrids seem to be a useful tool to keep electric systems controlled in a reliable way, the combination of them is a very attractive way to investigate.

Commercial buildings, schools and hospitals can be used as testing facilities for the combination of microgrid and microturbine. The main reason is that different variations of electric loads can exist there, and they can be daily, monthly or even seasonal.

In some previous works, the scheduling of the microturbine operation has been examined and confirms that the cost of microturbine use comes only from fuel consumption, what means that in case of having a favourable tariff of gaseous fuel, the microturbine is a very good solution for an effective primary source of the microgrid.

Currently, the microgrid with the microturbine operation has been successfully tested, especially in commercial and isolated installations. Now it is the moment to expand the use of this combination in industrial areas, bearing in mind that it can be advantatgeous for decentralised energy production.

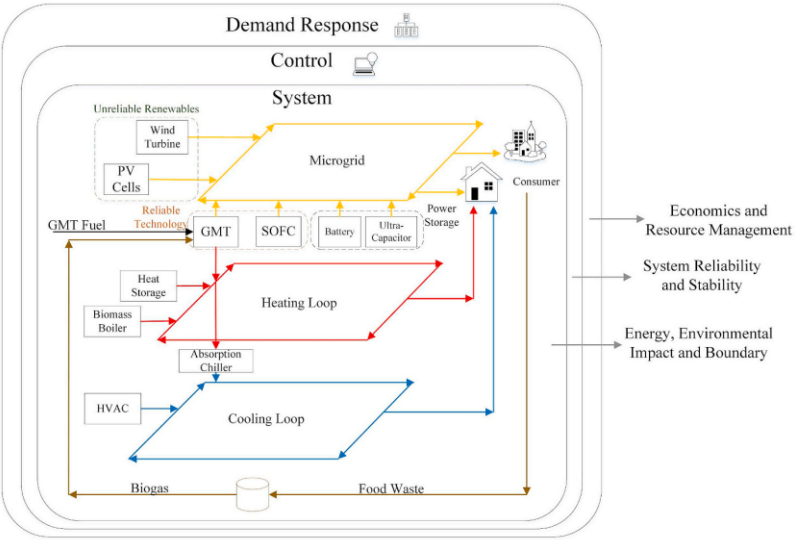

Figure 1.9: Microturbine-based microgrid system, control and demand response [8].

In Fig. 1.9 the incorporation of the microturbine to a microgrid can be seen. It is important to note the compatibility of microturbine and other renewable energy source, so the system is ready to operate in almost any condition. Also, note the classification of them. Whileas the wind turbine and the PV cells are considered to be unreliable sources, the GMT (Gas Microturbine) is considered to be reliable.

Microturbine-based microgrids are known for their support in remote areas, the help with the peak-shaving and the stabilization of market prices. They are controlled systems which main goal is to respond to demands, providing the adequate energy security. And as previously mentioned, the ease of working with low maintenance and good controllability makes the microturbine a suitable prime mover.

1.5 Recent applications

Some applications that have been performed during last years are explained below. Note that they are projects that have been carried out in very different environments, what shows the flexibility and adaptability of microturbine systems.

Felsineo La Mortadella

Felsineo is one of the leading producer companies of quality meats. It was founded in 1947 in Bologna, Italy. The business grew up and started to produce many types of meat and to export them. Therefore, they decided to improve the power gener-

ation system in order to increase their production, their operational efficiency and reduce their carbon footprint.

It was in 2014, when Felsineo decided to install a combined heat and power system (CHP) to recover the thermal energy and convert it into steam for making mortadella. Then, *Capstone Turbine Corporation* installed a natural gas-fueled microturbine along with a compressor and a postcombustion steam generator solution.

The installed microturbine was coupled with a post-combustor burner and steam boiler, what allow them to obtain the necessary steam at the required pressure. This improved significantly the operational efficiency. Also, the microturbine generates the 1 MW of power to ensure the electrical load of the facility is comfortably met.

Figure 1.10: The natural gas-fueled C1000 microturbine was installed onsite along with a gas compressor and postcombustion steam generator solution [9].

Felsineo is the first microturbine project of Capstone where they performed a post-combustion steam solution, which satisfied both the electrical and thermal demands of the facility. The overall efficiency obtained is greater than 80%. Thanks to that, Felsineo is saving about 300.000 € per year of operation costs. This also means that they are avoiding to release 478 tons of CO_2 to the atmosphere. Therefore, this was an important project for both companies, where the resulst were more than satisfactory.

Utility Software Company

In this case, the type of business that is supported by microturbine systems is involved in microgrids. Microgrids represent an energy distribution market that is growing in a fast way and new opportunities to get higher performance efficiencies arise every day.

The fact of guarantee reliable power for the mission-critical data center was the main priority in this work for Capstone. Since many years ago, data centers rely on power from the utility and they count on banks of batteries to keep the servers and the equipment running in emergency cases.

In this case, the microturbine is configured to provide power and thermal energy in the event of a grid failure in autonomous way. The model used in this case is a C600S microturbine which is a dual mode model, capable of operating connected to a utility grid or operate stand alone, providing power to critical loads when the utility is unavailable. The microturbine is controlled by two redundant controllers for maximum resistance.

Figure 1.11: Natural-gas-burning microturbine system with heat exchanger form the backbone of the microgrid for the office building and data center [10].

The Capstone C600S microturbine is always in operation. The output is adjusted by the microgrid controller to coordinate with the solar and wind power generation to provide a great economic profitability. The customer may expand the microturbine package as the building load increases and that would be possible without modifying the original microturbine system.

This application is the perfect example to show that microturbines are able to be implemented and work in a variety of fields that are rapidly growing.

1.6 Brief background of the company involved in the current study

Compower AB is a technical consultant company, based on Sweden. It is currently working on developing new ways to generate both heat and power in private homes.

Compower AB was founded in 2004, based on the wide experience of the founders, industrial research and development of small, turbine-based power-generating systems. Originally based out of Lund and Glimåkra in Skåne, the operation has now mostly moved to the Royal Institute of Technology in Stockholm where research is done at the labs of the Department of Energy Technology.

Compower made pioneering work on the integration of micro turbines and electric generation systems. Its research is a part of the larger umbrella project Explore Polygeneration, a European Union financed project to link together the latest research in the Energy field.

1.7 An example of previous models developed by Compower AB

In this section one of the original models of microturbine that Compower AB has developed until now is going to be explained. It is important to note that all the elements of its microturbines have been manufactured by other companies, which means that all of them are commercialized models. So no calculations about the flow through the several passages nor any three dimensional analysis have been performed previously.

In the Fig. 1.12 we can see that there are 8 stations where the flow can be defined. The parameters we know about the flow are temperature, pressure and mass flow. The inlet conditions in the station 1 are known values, so to calculate the following stations the necessary mass and energy balances have been performed. For that, the manufacturers data from the compressor, recuperator, turbine and combustion chamber have been considered.

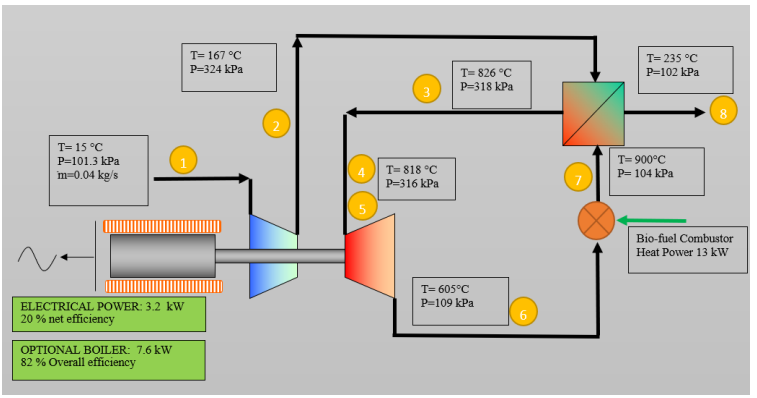

Figure 1.12: Thermodynamic cycle of the original model developed by Compower AB, the shown values are only representative values of many simulation cases.

Here is a brief explanation about the flow path. The flow comes into the microturbine from outside at atmospheric conditions. It passes near the electrical generator and enters the compressor. Note that the generator, the compressor and the turbine are attached in the same shaft. Afterwards, in station 2 the compressor has increased the pressure thanks to its compression ratio of 3.2. The flow enters into the recuperator and there is a heat exchange with the combustion chamber outlet. In station 3, the flow has notably increased its temperature. Stations 4 and 5 represent the the volute and the nozzle row. Through them both the temperature and the pressure decrease. Station 6 is the turbine outlet and the flow is directed towards the combustion chamber. As a result, we get station 7, with a higher temperature and a bit lower pressure. The last phase is the heat exchange in the recuperator just before the exhaust in station 8.

Also, it is good to consider the obtained power from the turbine. The net output power in this case is 3.2 kW, that is extracted from the generator. This is the result of the subtraction of the required power for the compressor to the obtained power from the impeller rotation.

2

Objectives and methodology

This chapter presents the objectives of performing this research work and the methodology followed to achieve the goals. The design constraints, the working fluid and operating conditions of the microturbine are also presented here.

2.1 Objectives

The main objective of this project was to design a radial inflow microturbine that is going to be part of a heat and power generation unit for domestic use. Therefore, the goal of this project is to create the initial profile of the blades for the radial inflow turbine. A non-dimensional analysis and a previous study are necessary to understand the parameters and equations on which the design is based. Afterwards, a preliminary design will be performed and this will ease the final design of the microturbine. Therefore, two main steps are foreseen:

- Analysis of radial turbomachines and study of the involved equations and parameters.
- Design and generation of the flow passage based on the given operation conditions.

The steps above are interconnected. The first one involves more theoretical aspects, whileas the second one is referred to the parameters in the same way as in the software and in the book of Ronald H. Aungier [3]. Note that the first step will be especially important in order to perform the aerodynamic design of the radial inflow microturbine as accurate as possible.

2.2 New model of the microturbine

Before explaining the initial parameters it is good to know that this research work was initiated by Compower AB to design a microturbine for a heat and power gen-

eration unit for private houses. Since 2014 they have been developing several prototypes and testing them in Malmö as well as in Stockholm. Bearing in mind that the efficiency levels could be better, it is intended to perform a more efficient and a better design for the coming prototypes.

Working conditions

Compower AB provided with the working conditions of the microturbine to start the design process. These values are shown in Table 2.1.They are the initial input data when performing the One-dimensional Aerodynamic Design that is explained in the following chapter.

Table 2.1: Working conditions for the 100% load case. These are the main characteristics of the microtubine.

Property	*Value*	*Units*
Net Output Power	3.5	kW
Mass Flow Rate	3	kg/min
Inlet Total Temperature	900	ºC
Inlet Total Pressure	2.648	bar
Pressure Ratio	2.536	-
Outlet Total Pressure	1.044	bar

These values are from the case in which the turbine is giving the 100% of the output power. The design of a turbine has to be always performed considering the 100% loading. This will be the operating point of the turbine. However, sometimes the turbine will work at off-design points. These are other running points that do not match the operating point.

At 50% load the rotational speed is reduced to achieve correct mass flow and pressure ratio. The inlet turbine temperature is kept high to get the best part load efficiency. This is the advantage when having a high speed generator connected to an electrical converter. This means that the generator speed can vary and still get 50 Hz electrical output. In a different way, for a traditional gas turbine with gear box and synchronous generator, the only way to get part load is to reduce the turbine inlet temperature. [personal communication , Compower AB, 2021].

The working medium in the system is air. Its behaviour can be approximated by the ideal gas law and the turbine exhausts to atmosphere. This will be very helpful when performing the design since aproximations following the ideal gas relation will be able to be performed. Note that the outlet total pressure in Table 2.1 is referred to the outlet of the impeller.

The working cycle

Here the thermodynamic cycle in which the radial-inflow microturbine is going to work is presented. The main elements such as the compressor, the heat recuperator, the combustion chamber, the microturbine and the generator are shown.

When comparing the current working cycle shown in 2.1 with the one from the previous turbine model from Compower AB previously shown in 1.12, a big difference can be seen. It is the order in which the turbine and the combustion chamber are located.

In the previous model the combustion chamber, also called combustor, is located just after the turbine. This means that the main inlet of heat input takes place once the flow has left the turbine. Afterwards, it goes to the heat recuperator and then to the turbine. In this case, the combustion chamber is located before the inlet of the microturbine. The recuperator is used as a heat exchanger between the outlet of the compressor and the exhaust flow after passing through the turbine.

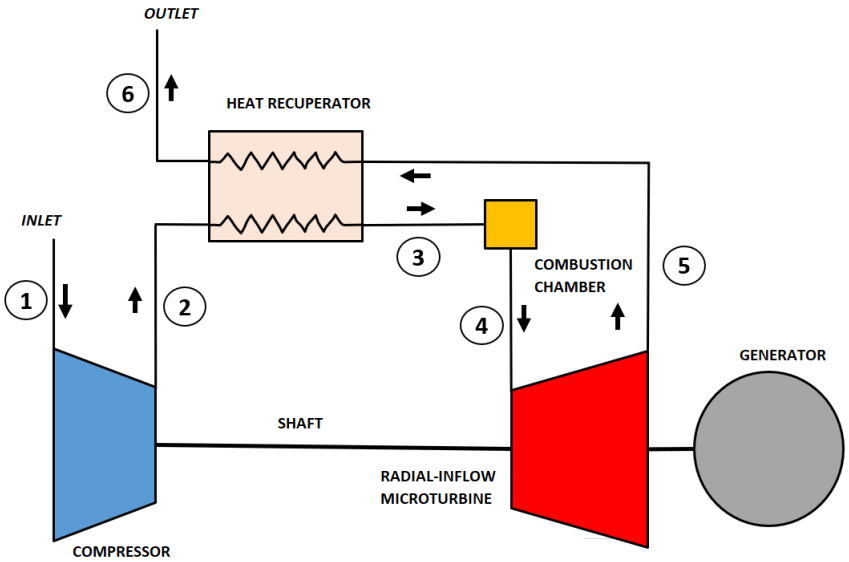

Figure 2.1: Working cycle of the radial-inflow microturbine. Compressor, combustion chamber, microturbine, generator and recuperator are represented.

Figure 2.1 shows a basic scheme of the working cycle. The points represent each flow state between different phases. In this case, the radial-inflow microturbine shown in the picture represents the group of elements that will be designed in this work. This means that the element called ”radial-inflow turbine” in the picture involves the volute, the nozzle vanes, the impeller, the diffuser and the vaneless passages.

Limitations

Some limitations have arisen in the design process that are listed below:

- **Rotational speed:** In some previous models the rotational speed has been an issue since it is strongly coupled with the mechanical aspect of the shaft. The main cause of this phenomenon is that the compressor and the turbine are in the same side of the shaft, so they are not well balanced. Therefore the constraints based on the working conditions require that the roational speed are limited to the 200000-230000 (rpm) interval.

- **Blade thickness distribution:** There are also some constraints imposed on the blade thickness distribution. The experience has led Compower AB to perform a graph that shows the relationship between the blade thickness in the hub and in the shroud. It is shown in Fig. 2.2. It shows that in the widest section of the blade, the thickness of the hub has to be approximately three times more the thickness of the shroud. Note that this is a simplified representation of the blade since only 6 sections are used. In the current design, a larger number of sections of the blades will be used in order to get a higher accuracy.

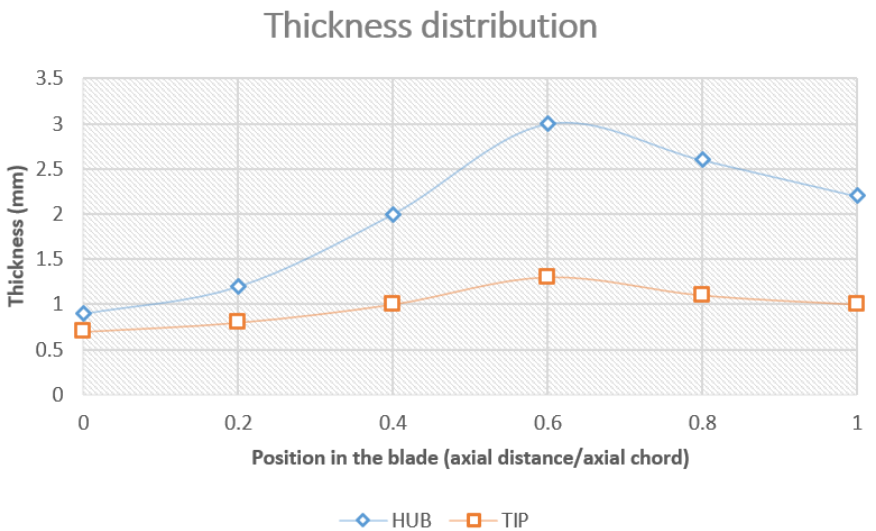

Figure 2.2: Experience has led Compower AB to make a graph that shows the relationship between the blade thickness in the hub and in the shroud. [Compower AB, 2021]

2.3 Methodology

In this section the project phases and the connections between them are explained. The work is carried out based on the following methodology:

1. Literature survey through browsing among recent studies in the field of radial-inflow turbines in opes publications.

2. Study and understanding of how the system works. Visualization of the drawings of the previous radial inflow turbine designed by Compower AB. It is important to identify the most important parameters that affect the performance of the turbine and how they are related.

3. Detailed analysis of the main groups of non-dimensional equations, as well as of the dimensionless parameters required for turbine type selection.

4. Preliminary design based on the working conditions specified by Compower AB. These conditions are shown in Table 2.1. For this preliminary design a TurbAero software package called RIFTSIZE will be used.

5. Aerodynamic design and generation of the blade geometry of the turbine using tools provided by TurbAero software. It has a wide package with several programs that are used for getting different design data for components of the radial turbine. The functions of the packages and the relations between them are explained in a more detail in the next chapter.

6. Finally, the resulting plots and drawings obtained from the aerodynamic design will be shown and commented in order to provide a good visualization of the main elements of the designed microturbine.

3

Governing equations

This chapter gives a general overview about the most important equations that are involved in the behaviour of the flow all along the turbine. Also these equations are highly related to the development of the calculations performed by the software TurbAero.

Fluid state equation

In this chapter w means relative velocity and ω means rotational speed. Some subscripts have been used and their meanings are as follow: 0 total; 1 inlet stator; 2 outlet stator and inlet rotor; 3 outlet stator; n normal; x axial; and θ tangential.

The equation of state of the perfect gases relates in a very simple way the fundamental variables with which their behavior is modeled. P is the pressure, ρ is the density, T is the temperature and R is the universal constant for perfect gases.

$$P = \rho RT \tag{3.1}$$

Air is going to be the fluid flowing through the turbine. The air composition consists of a 78% of nitrogen and a 22% of oxygen. The molecular weigh of nytrogen (N_2) is 28 g/mol. The molecular weight of oxygen (O_2) is 32 g/mol. Therefore the molecular weight of the air can be calculated as:

$$M_{air} = 0.78 * 28 + 0.22 * 32 = 28.88 g/mol \tag{3.2}$$

In order to obtain the gas constant for air, the universal gas constant must be divided by this molecular weight.

Coordinate system

In order to describe and analyze the motion of a fluid inside turbines, cylindrical coordinates are used. In these coordinates, the axial component, the radial component and the angle in relation to one of the axes are specified. Likewise, this coordinate system is usually used when designing turbine components, especially impellers. It is really useful since the axial coordinate is almost always on the axis of rotation. Fig. 3.1 shows both the Cartesian and cylindrical coordinate systems.

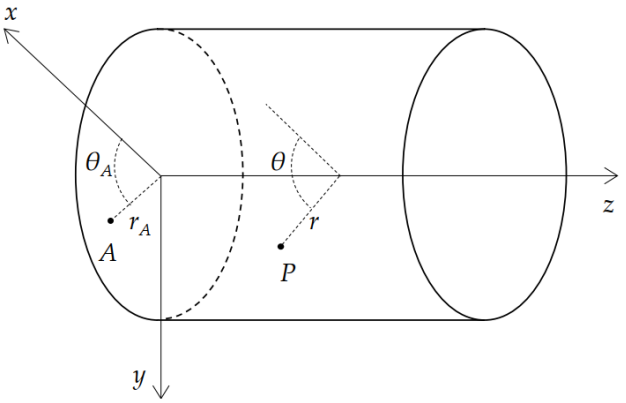

Figure 3.1: Cylindrical coordinate system to describe the trajectory of a fluid particle, as well as the turbine components geometry. Here the z coordinate is on the axis of rotation [11].

Conservation of mass

Here the main basic equations that explain the conservation of mass in a system are shown. The content of this section is based on [12]. The sum of the mass flow rates over all the system boundaries is equal to the change in mass in the control volume:

$$\sum_i \dot{m} = \frac{\delta m}{\delta t} \tag{3.3}$$

In the case of having a steady process, the mass in the control volume along the time is equal to zero, $\frac{\delta m}{\delta t} = 0$, therefore:

$$\sum_i \dot{m} = 0 \tag{3.4}$$

The mass flow can defined as:

$$\dot{m} = \rho \cdot c_n \cdot A \tag{3.5}$$

And considering the following control volume, where the indexes "1" and "2" refer to the inlet and the outlet respectively:

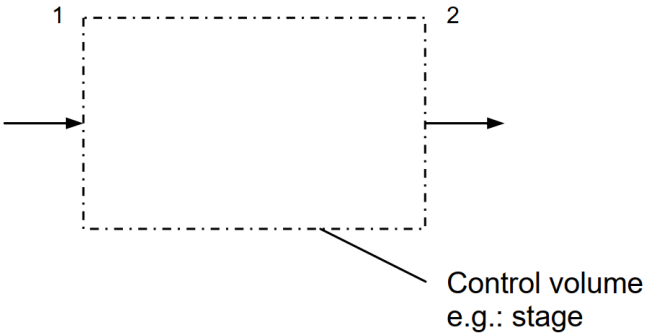

Figure 3.2: Control volume for mass flow system.

Both the inlet and the outlet can be matched in the following way:

$$\rho_1 \cdot c_{n,1} \cdot A_1 = \rho_2 \cdot c_{n,2} \cdot A_2 \tag{3.6}$$

Conservation of energy

The conservation equation for energy is described here. For a complete cycle and closed processes, the first law of thermodynamics states:

$$\oint (dQ - dW) = 0 \tag{3.7}$$

Then, when there is change between one point to another in the cycle, the internal energy is:

$$dE = dQ - dW \tag{3.8}$$

When the process is steady, the conservation of energy per unit time is considered:

$$d\dot{E} = \dot{m}(dh_0 + g \cdot dz) = \dot{Q} - \dot{W} \tag{3.9}$$

Where dh_0 means the change in the total enthalpy and $g \cdot dz$ is the change in potential energy. Moreover, if the process is assumed as adiabatic and steady, the conservation of energy for a turbomachine process can be written as:

$$\dot{W} = \dot{m} \cdot (h_{01} - h_{02}) \tag{3.10}$$

And it is important to see the difference between:

- turbines (work producing machines) $\Rightarrow \mathrm{h}_{01} > h_{02} : \dot{W} > 0$
- compressors and pumps (work consuming machines) $\Rightarrow \mathrm{h}_{01} < h_{02} : \dot{W} < 0$

Conservation of momentum

The following equations describe the moment of momentum balance and its conservation. The subindex 1 and 2 are referred to two different states of the fluid. They are referred to the inlet and the outlet of the turbomachine respectively. The sum of all the forces on a body is equal to the change of the momentum according to Newton's second law:

$$\sum F_X = \frac{\delta m c_x}{\delta t} \tag{3.11}$$

In case of having a steady process, the only cause of the momentum change is the change in flow velocity:

$$\sum F_X = \dot{m} \cdot (c_{x1} - c_{x2}) \tag{3.12}$$

Note that based on Bernouilli, a change in velocity means a change in the pressure for an incompressible fluid:

$$p_0 = p + \frac{1}{2}\rho \cdot c^2 \tag{3.13}$$

Note that for a compressible fluid the ideal gas relations for isentropic flow must be used to relate the total and static properties. Then, the moment of momentum that really matters in turbomachinery is:

$$\sum M_z = \sum r \cdot F_\theta = \frac{\delta (r m c_\theta)}{\delta t} \tag{3.14}$$

Finally, in case of a steady flow process, the tangential flow velocity causes the change in moment of momentum:

$$\sum M_z = \dot{m} \cdot (r_1 c_{\theta 1} - r_2 c_{\theta 2}) \tag{3.15}$$

Euler's turbine equation

The following equations represent the behaviour of fluids in motion and the most important parameters. They combine the conservation of energy and the conservation of moment of momentum. The product of moment and rotational speed equals the mechanical work per unit time:

$$\dot{W} = M_z \cdot \omega \tag{3.16}$$

Therefore, both the conservation of energy and the conservation of momentum can be related in the following way:

$$\dot{m} \cdot (h_{01} - h_{02}) = \dot{m}(r_1 c_{\theta 1} - r_2 c_{\theta 2}) \cdot \omega \tag{3.17}$$

Then, eliminating $\dot{m}$ and substituting $r \cdot \omega$ by the tangential speed u, the Euler's turbine equation is obtained:

$$h_{01} - h_{02} = u_1 c_{\theta 1} - u_2 c_{\theta 2} \tag{3.18}$$

When reformulating Euler's turbine equation, a fundamental aspect for turbomachinery is obtained. It is known as rothalpy and comes from the following equation:

$$h_{01} - u_1 c_{\theta 1} = h_{02} - u_2 c_{\theta 2} = I \tag{3.19}$$

And the general notation of rothalpy is:

$$I = h + \frac{1}{2}c^2 - u \cdot c_\theta \tag{3.20}$$

Considering the velocity triangles that relate absolute, relative and tangential velocity so that $\vec{c} = \vec{u} + \vec{w}$, the rothalpy can be expressed as:

$$I = h + \frac{1}{2}w^2 - \frac{1}{2}u^2 \tag{3.21}$$

The velocity triangle that relates these factors has the following shape:

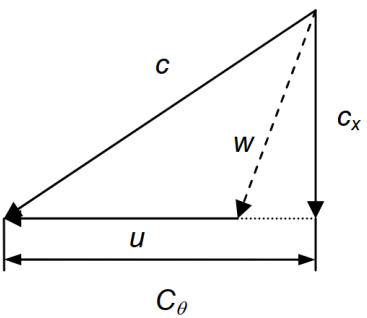

Figure 3.3: Velocity triangles for turbomachinery.

Compressible relations

Here some of the most important parameters regarding compressible flow machines are defined. The equations of this type of machines deal with variable density flow. Many fluids with small density variations use incompressible fluid equations. Bernoulli's equation is very used in this case.

$$p_0 = p + \frac{\rho}{2}c^2 \tag{3.22}$$

The Mach number is a measure of significance and it is used to relate the flow speed with the speed of sound as follows:

$$M = \frac{c}{a} \tag{3.23}$$

The Mach number sets the relation between the total and static properties (e.g. Pressure, Temperature, etc) for a compressible fluid.

In addition, the speed of sound can be defined knowing some parameters of the fluid where the sound wave is going to be transmitted. These parameters are shown in the equation below:

$$a = \sqrt{\gamma RT} \tag{3.24}$$

Finally, the Mach number can also be used in isentropic relations for perfect gases:

$$M = \left[\frac{2}{\gamma - 1} \left[\left(\frac{p_0}{p} \right)^{\frac{\gamma-1}{1}} - 1 \right] \right]^{\frac{1}{2}} \tag{3.25}$$

4

Dimensional Analysis

In this chapter a performance analysis will be carried out at the inlet and outlet of the turbine components (volute, nozzle, impeller, vaneless spaces and diffuser). The analysis is based on several thermodynamic and aerodynamic relations. The main non-dimensional groups for both incompressible and compressible machines are explained. Also, the specific speed and the specific diameter are explained considering that these are generally the most important parameters when selecting the type of turbine to be used.

4.1 Non-dimensional groups

This section will consist on showing the main expressions and relations of the most representative parameters in the design of a radial turbine for both cases imcompressible and compressible flow. Incompressible flow machines are easier to deal with than compressible flow machines since the properties of the fluid do not change significantly. Also, some machines in which the density variation of the fluid is very small can be considered as incompressible when talking about performance characteristics.

Incompressible flow

Based on Baines [2], the power P, the volume flow rate Q, the rotational speed N, and the head change $g\Delta H$, are the operational parameters in which the performance characteristics can be expressed. Moreover the diameter D represents the size of the machine and the density ρ and viscosity μ represent the fluid properties. Therefore, the relation between these properties can be written as follows:

$$P = f(Q, N, gH, D, \rho, \mu) \tag{4.1}$$

The equation above is just an example of the relation between the parameters shown. It has been written with the power, since it is often one of the targets to achieve in the turbine design. Anyway it would be possible to write it in the same way for others.

Applying the Buckingham Pi theorem [1] and considering all the parameters of the equation 4.1 we can have four dimensionless groups [2]:

Power coefficient: $$P = \frac{P}{\rho N^3 D^5}$$

Flow coefficient: $$\phi = \frac{Q}{ND^3}$$

Head coefficient: $$\psi = \frac{g\Delta H}{N^2 D^2}$$

Reynolds number: $$Re = \frac{\rho N D^2}{\mu}$$

The functional relationship between these groups is:

$$\frac{P}{\rho N^3 D^5} = f\left(\frac{Q}{ND^3}, \frac{g\Delta H}{N^2 D^2}, \frac{\rho N D^2}{\mu}\right) \tag{4.2}$$

or

$$P = f(\psi, \Phi, Re) \tag{4.3}$$

In many cases it is possible to neglect the Reynolds number, because experience shows that it has much less influence on the performance than the other groups. If this is done, equation 4.3 is simplified to:

$$P = f(\psi, \Phi) \tag{4.4}$$

The second expression that defines the flow coefficient is also called velocity coefficient and it is commonly used in non-hydraulic turbines, where U is the mean blade speed and c_m is the average meridional velocity. Another operational parameter that may result really interesting in order to compare the performance of several

[1] *Buckingham Pi Theorem*: (number of independent dimensionless groups required to be equivalent to the set of physical parameters)=(number of physical parameters)-(independent fundamental units)

turbines is the efficiency. This can be expressed using the previous dimensionless groups:

$$\eta = \frac{\mathbf{P}}{\phi\,\psi}$$

Compressible flow

In compressible fluids the application of dimensional analysis to turbines can be more complicated, since the properties may not be considered constant along the components. Note that the working fluid used in this work is air, what means that we are considering the relations and coefficients for a compressible flow that are described below.

The coefficients explained can be either directly or indirectly affected by density changes. Then, it is necessary to express the compressible flow machine performance using other parameters that are related in the following way:

$$p_{01} = f(p_{03}, T_{01}, T_{03}, m, N, D, R, k, \mu) \tag{4.5}$$

Note that in equation 4.5, temperature and pressure values are referred to different stations (1: inlet and 3: outlet) of the stage so that the density has different values in each of them. Then, the dimensionless groups to consider for compressible flow machines are as follows [2]:

Pressure ratio: $\frac{p_{01}}{p_{03}}$

Temperature ratio: $\frac{T_{01}}{T_{03}}$

Mass flow coefficient: $\frac{m\sqrt{RT_{01}}}{p_{01}D^2}$

Speed coefficient: $\frac{ND}{\sqrt{RT_{01}}}$

Reynolds number: $\frac{p_{01}ND^2}{RT_{01}\mu}$

Specific heat ratio k (a physical parameter, but already dimensionless).

The mass flow coefficient, the speed coefficient and the Reynolds number are expressed in terms of the inlet conditions in this case. Bearing in mind the constant

change of the density, they could be expressed in the same way in terms of the outlet conditions [12].

The dimensionless groups shown until now are the most representatives and the most used when analysing radial turbines. Nevertheless, depending on the working parameters and which of them are known or unknown other non-dimensional groups can be used. The work coefficient, the blade speed ratio and the machine Mach number are some of them.

Flow coefficient and stage loading

Dixon [12] states that there are two key non-dimenssional groups for the design and analysis of a radial turbine working with compressible flow. These are the flow coefficient and the stage loading.

The flow coefficient is defined here in the same way as before for the incompressible flow machines, i.e. ϕ=c_m/U. The difference is that for compressible flow it can notbe used to fix the operating conditions since it depends on other non-dimensional parameters. The equation of state for perfect gases p/ρ=RT is used to define the density. Also it is good to know the relation of specific heats $\gamma = C_P/C_V$.

Note that the difference between the non-dimensional mass flow, $\dot{m}\sqrt{C_P T_{01}}/D^2 p_{01}$ and the flow coefficient, ϕ is that the first one does not involve the blade speed. Therefore, the flow coefficient is defined as:

$$\phi = \frac{c_m}{U} = \frac{\dot{m}}{\rho_{01} A_1 U} = \frac{\dot{m} R T_{01}}{p_{01} A_1 U} \propto f\left\{ \frac{\dot{m}\sqrt{C_P T_{01}}}{D^2 p_{01}}, \frac{QD}{\sqrt{\gamma R T_{01}}} \right\} \tag{4.6}$$

On the other hand, there is the other key non-dimensional group for compressible flow machines. This is the stage loading and it is really similar to the head coefficient ψ in incompressible machines. It is defined as:

$$\psi = \frac{\Delta h_0}{U^2} \tag{4.7}$$

While stage loading is a non-dimensional form of the actual specific stagnation enthalpy change, the head coefficient is a non-dimensional measure of the isentropic work that can be reached by an incompressible flow machine. In the same way as for the flow coefficient, the stage loading can be related to other non-dimensional parameters:

$$\psi = \frac{\Delta h_0}{U^2} = \frac{C_P \Delta T_0}{C_P T_{01} U^2} x \frac{C_P T_{01}}{U^2} = f\left\{ \frac{\dot{m}\sqrt{C_P T_{01}}}{D^2 p_{01}}, \frac{QD}{\sqrt{\gamma R T_{01}}} \right\} \tag{4.8}$$

Finally, considering that the stage loading is equal to the function that depends on the non-dimensional mass flow , $\dot{m}\sqrt{C_P T_{01}}/D^2 p_{01}$ and the non-dimensional blade speed, $QD/\sqrt{\gamma R T_{01}}$ it can be fixed once these both are fixed. The non-dimensional blade speed is also called blade Mach number.

4.2 Specific speed and specific diameter

The previous dimensionless groups can be replaced with a linear combination of other groups. Considering them, there are also two other parameters that can have a big repercussion when designing radial turbines and they are the specific speed and the specific diameter.

When choosing a turbomachine, no assumptions about the turbomachine itself should be made, and this means that a dimensionless group that does not include the size of the machine is needed. The parameter that determines the size or the geometry of it is the diameter. Therefore, the dimensionless groups that accomplish this requirement are the ones of the specific speed. It is function of the volume flow, the rotational speed and the head change. It can be written in several ways, but the most common is shown in the following expression:

$$N_s = \frac{\omega\sqrt{Q}}{(g\Delta H)^{3/4}} \tag{4.9}$$

Equation 4.9 is used for design and selection of low speed and incompressible flow turbines. And the concept of specific speed can be applied to a compressible flow machine as well. It is really important when the decision of going for an axial or a radial turbine comes.

Then, since a large variation in the volume flow rate, Q, and the head, H, exists in compressible machines, a modification is necessary. Therefore, the specific speed for compressible and high-speed turbomachines is expressed as:

$$N_s = N\left(\frac{\dot{m}}{\rho_e}\right)^{1/2}(\Delta h_0)^{-3/4} \tag{4.10}$$

In equation 4.10 the subindex e means exit, which means that the density is referred to the outlet of the turbine. This can be obtained from the equation of state $\rho_e = p_e/RT_e$, where p_e and T_e are taken from the exit of the turbine.

Bearing in mind that the equations 4.9 and 4.10 do not have any reference to the size or the geometry of the turbomachine, another dimensionless parameter is used. It is the specific diameter. It depends on the diameter, the head change and the flow. It does not consider the speed of rotation. The most common expression to define it is the following:

$$D_s = \frac{D(g\Delta H)^{1/4}}{\sqrt{Q}} \tag{4.11}$$

Both the specific speed and the specific diameter are related through charts. One of them has been very used over many years and is shown in the Fig. 4.1. It is based on the behaviour of water turbines and pumps. The bold line in the graph is known as the Cordier line and shows the trend of the well designed machines. The line and arrows show the limits and the zones for a specific turbine design, e.g. the left of the

bold line is more suitable for radial turbomachines. It is important to note that this chart is only a good starting point for general developing of turbomachines, since it was performed for machines that are not very common nowadays.

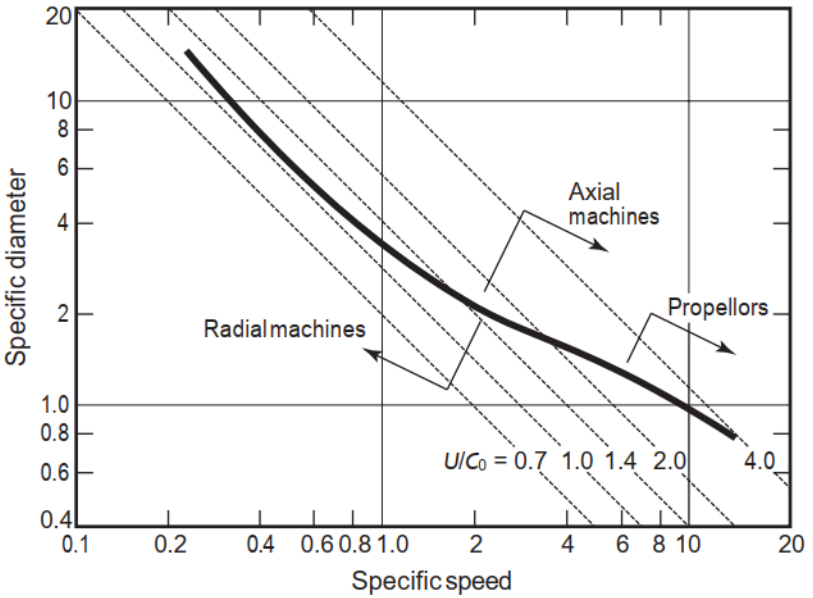

Figure 4.1: Diagram of specific speed and specific diameter for "well designed" turbomachines. It has additional lines for the values of U/C_0 [2].

Radial turbine selection

As shown in Fig. 4.1 the specific speed and the specific diameter are usually the dimensionless groups that are used as starting point for when the turbomachine has to be decided.

Several researchers have documented the relation that the non-dimensional diameter and specific speed have with the type of turbomachine selection through extensive experiments and experience.

In Fig. 4.2 not only the specific speed and the specific diameter are used to determine the type of turbine, but also the U/C_0 ratio and the efficiency. The U/C_0 ratio is represented by the lines that cross diagonally the graph. The efficiencies are represented by the curved lines showing this way different areas with different efficiencies.

It is also said that Ns-Ds diagrams are used for determining the performance of a turbomachine knowing the specific application. They are used for compressors, pumps and turbines. In the case of turbines, the volume flow is referred to the exit.

And in order to determine it, an efficiency level is assumed.

Now, when the efficiency value is decided, the minimum value of Ns for this efficiency is obtained on the Ns-Ds chart. Afterwards, in the Ns equation, the value is substituted and the rotative speed can be known. On the other hand, for most applications the value of the roative speed will be determined by stress levels, maximum bearing or gear speeds. For instance, in the case of pumps, the cavitation phenomenon usually determines the rotation speed.

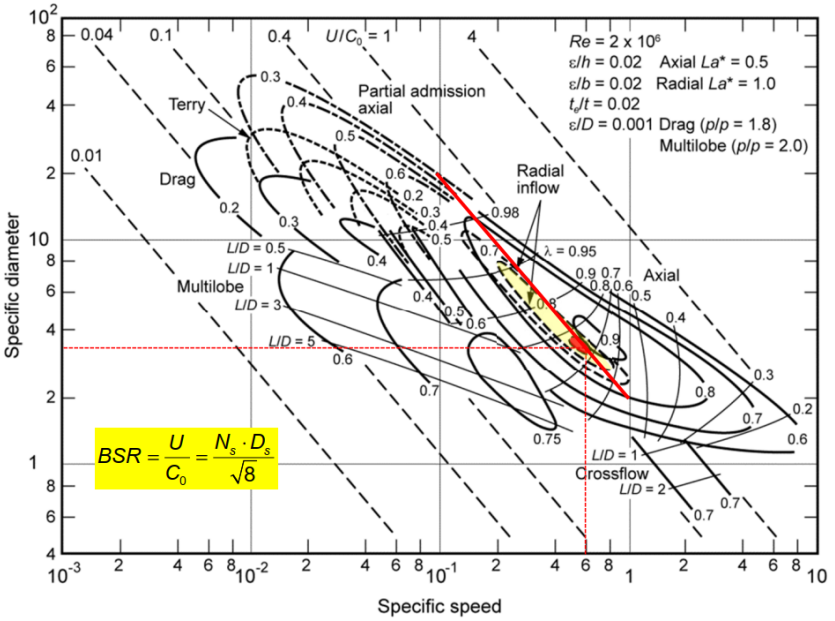

Figure 4.2: Diagram of specific speed and specific diameter used for the radial turbine selection [13].

As explained in section 2.2, the main cause that determined the rotational speed between 200000-230000 rpm was the maximum bearing due to the location of the turbine and the compressor. Anyway, the Balje chart for turbine selection shown in Fig. 4.2 has been used as starting point for that and it is always strongly recommended.

5

Aerodynamic design of radial turbine

In this chapter the one and two-dimensional design of the microturbine stage is going to be performed. It will be carried out at the inlet and outlet of the turbine components (volute, nozzle, impeller, vaneless spaces and diffuser). Depending on the inlet conditions of the stage, predictions of geometrical parameters will be obtained. Radius, blade angles, blade thickness and surface coordinates are some of them. Note that the operating conditions in which the design will be based on are shown in Table 2.1.

5.1 Introduction to TurbAero

Here the tool used to perform the one- and two-dimensional design is going to be described. It is called TurbAero and it is a software that implements the aerodynamic design and analysis for axial and radial-inflow turbines. All the models and the codes used are based on the R. H. Aungier's book [3] including the default values. During this work some of the initial values have been left as default. TurbAero has several working packages and many of them can be used for both compressors or turbines. The most used programs from TurbAero in this work are explained below [14]:

- **RIFTSIZE** *(Radial-inflow turbine size)*. This is the first program to be used to design in a preliminary radial-inflow turbine stage. One-dimensional thermodynamic equations and empirical correlations are used here. It is possible to input the basic parameters of each component of the stage. After that, it creates some results in both text and graphical documents and gives the input data to other programs that will carry out the detailed stage design. The programs that will work with these data are the following.
- **RIFT** *(Radial-inflow turbine)*. It works for single-stage or multistage radial-inflow turbines. Every component of the stage is calculated using three sta-

tions on a mean-line basis. It can also be used to modify some parameters in the middle of the design process and can update the input files for the programs B2B2D and TDB2B. This program has not been used to get output data to be used later in the geometry generation. Its role has been more related to support the work in the other programs.

- **RIFTNOZ** *(Radial-inflow turbine nozzle)*. This is specially developed for designing the nozzle rows of the radial-inflow turbine. To match the inlet and outlet velocity triangles, it uses a standard airfoil family. The input file here is supplied by RIFTSIZE and it can be used to create or update input files for B2B2D, TDB2B and RIFT. Note that this is the ususal approach to nozzle detailed aerodynamic design.

- **B2B2D** *(Blade-to-blade two-dimensional)* and **TDB2B** *(Time-dependent blade-to-blade)*. These programs work with the same input file and they most common goal they are used for is nozzle blade loading evaluation. B2B2D is appropiate for subsonic and low transonic Mach number levels. Whileas B2B2D is a two-dimensional flow method, TDB2B works with a time-marching method, which makes it suitable for any value of the Mach number. Therefore, the program TDB2B is mostly used when B2B2D cannot work with the input Mach number values.

- **GASPATH** and **BEZIER**. Its most common use is the design of radial-inflow turbine impeller. In GASPATH the hub and shroud contours and blades are designed. In BEZIER the curves used to construct the blades and end-wall contours are generated based on the Bernstein polynomials. The input files come from the program RIFTSIZE. This one is also used to obtain the coordinates in an output file. Program GASPATH can be very interesting to use when there is a base of the impeller geometry to work on. The hub and shroud contours can be modified until getting a satisfactory blade loading.

- **RKMOD**. It uses a wide database of gas properties and equations to calculate the flow properties that various programs need. Single-phase and mixture fluids can be calculatesd, and the composition of them can be chosen. RKMOD supports all the packages in TurbAero in the design and analysis of turbomachines. It also allows to compare its gas property predictions with others chosen by the user. It can be used for creating tables of thermodynamic property data among many others. In this work it has been used to select the type of fluid and to check all its parameters.

As stated before, these are the programs that have been used the most and it is also important to know which of them are related and the order in which they have been run in the iterative process of designing and analysing a radial-inflow turbine. The flow chart of the relation between various programs of TurbAero package can be seen in Fig. 5.1.

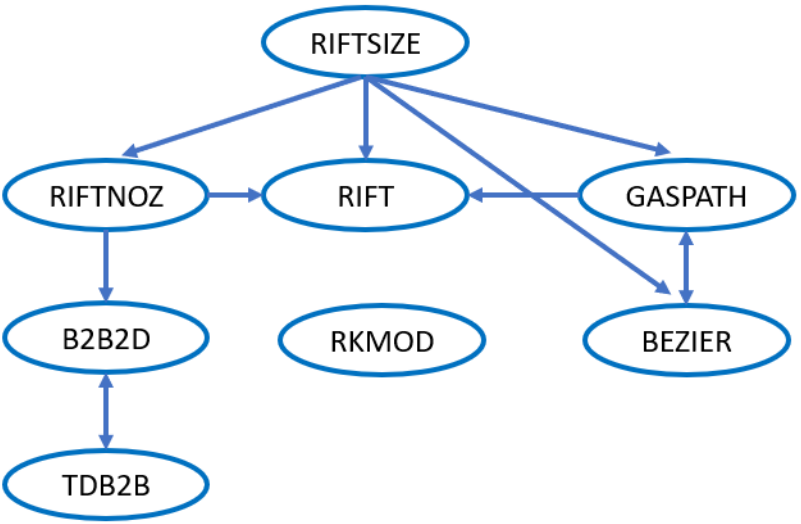

Figure 5.1: The most used programs of TurbAero and the relation between them in a design of a radial turbine process. Source: own elaboration.

In the following sections of this chapter the procedure followed through the design process with programs of TurbAero is explained as well as the obtained results in each of them.

5.2 Preliminary design using RIFTSIZE

Here the process and the most important parameters used in RIFTSIZE are going to be explained. This has been the first program where the input conditions have been introduced. These conditions are shown in Fig. 2.1. Note that the net output power is a working condition but not a input data, since the output power in the shaft of the turbine is an output that is obtained with RIFTSIZE. In Fig. 5.2 the power in the shaft as well as the values of several efficiencies can be seen.

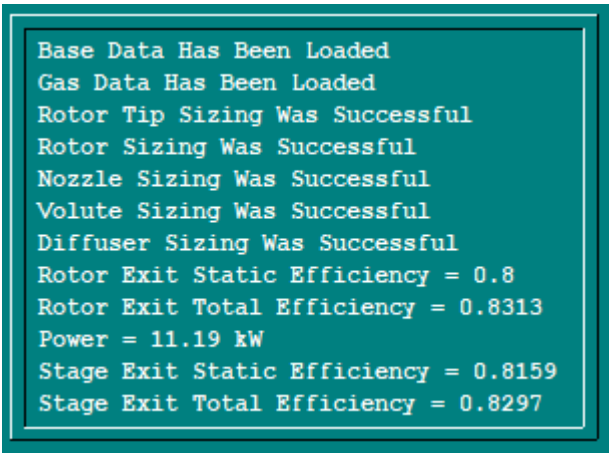

Figure 5.2: Basic output data obtained from RIFTSIZE

The output power from RIFTSIZE (11.19 kW) was very close to the power obtained using an Excel spread sheet solver that did similar performance calculations ons the same turbine set up. [Dept. of Energy Sciences, LTH, 2021]

There is another important parameter to consider here. It is the speed (rpm) of the shaft. Considering the recommended interval by Cpompower AB (200000-23000 rpm), it is better to go for lower values that are able to reach good values of efficiency. For this reason it has been decided to start with an assigned speed of 205000 rpm.

In RIFTSIZE it is possible to enter basic preliminary parameters for the rotor, the nozzle, the volute and the diffuser. In order to demonstrate the procedure followed in this thesis for the design of the radial turbine, some screenshots of the program are shown here:

- **Rotor.** In Fig. 5.3 all the preliminary input parameters and data for the rotor are shown. All the values in the grey gaps have been left per default. They are the values suggested by the program based on Aungier [3]. The number of blades is the only parameter that has been written following the instructions from Compower AB.

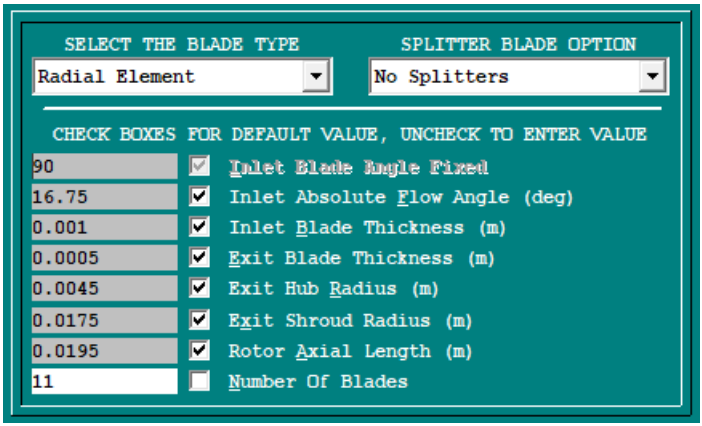

Figure 5.3: Preliminary input data for the rotor in RIFTSIZE.

- **Nozzle.** Figure 5.4 shows all the preliminary input parameters for the nozzle vanes. Here, in order to get a correct sizing the first two parameters and the exit blade pitch/chord ratio were chosen. In case there is any wrong parameter value, the program shows a warning until acceptable values are introduced. Since previous models of the company have had similar number of blades, Compower AB has decided to keep it.

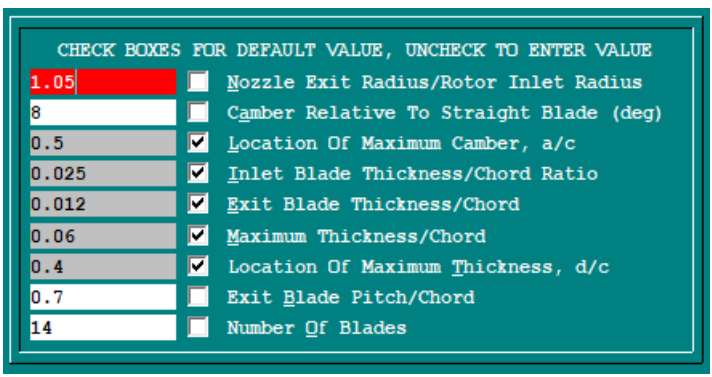

Figure 5.4: Preliminary input data for the nozzle vanes in RIFTSIZE.

- **Volute.** The preliminary parameters for the volute are very basic and the user is only allowed to choose the shape, the style and the geometric ratio shown in the bottom of Fig. 5.5. The selected value is 1, which means that the elliptical volute will have a circular cross-section.

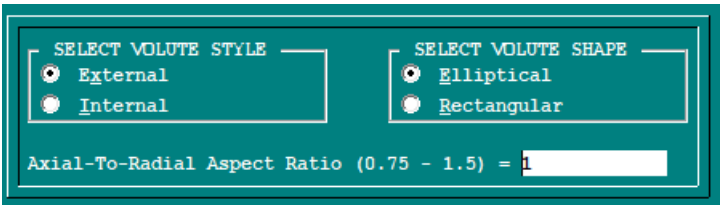

Figure 5.5: Preliminary input data for the volute in RIFTSIZE.

- **Diffuser.** The preliminary design of the diffuser is even easier than the volute one. Here the user is just selecting the area ratio between the inlet and the outlet as seen in Fig. 5.6. Instead of this parameter, the normalized length could be assigned.

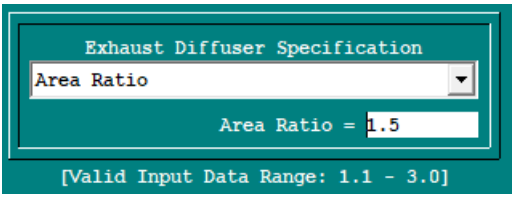

Figure 5.6: Preliminary input data for the diffuser in RIFTSIZE.

There are several results of introducing the input values and runing RIFTSIZE. The preliminary cross section of the stage can be seen in in Fig. 5.7.

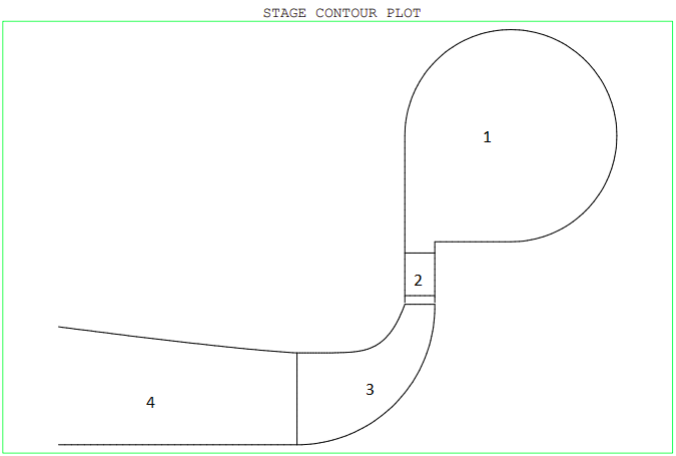

Figure 5.7: Stage half cross section from the output file of RIFTSIZE.

In Fig. 5.7 the different components of the radial turbine have been numbered in order to make more understandable the flow path. This way, the are defined in the following way:

1: Volute
2: Nozzle vanes
3: Impeller
4: Diffuser

Some other interesting data can be obtained from RIFTSIZE as the rotor contour and the nozzle cascade plots. However, here it is really important to consider the geometric coordinates of the rotor and the nozzle vanes, since they are going to be the input data for the 3D modelling of the turbine. They are given as polar coordinates, what means that a transformation to Cartesian system is necessary.

5.3 Design of the nozzle vanes using RIFTNOZ, B2B2D & TDB2B

The initial guide vane profile and loading distribution did not produce satisfactory results. Therefore it was decided that the guide vane parameters should be changed until satisfactory loading distribution can be obtained.

This way and bearing in mind that the preliminary results are not satisfactory, a detailed design that starts with RIFTNOZ is carried out. The blade loading plot plays here the most important role and getting the correct shape there, the guarantees of obtaining a correct behaviour of the flow through the blades are pretty high.

Since there were different points of view about the goal in the blade loading plot, a sharing of opinions has been necessary to get a conclusion. In Fig. 5.8 a blade loading plot is shown. This would be a good loading distribution of the blades. In this case only two parameters are specified: the blade camber angle θ and the distance to maximum camber/chord ratio a/c.

Onwards, the theory followed in this process is explained and also the characteristics that the blade loading plot should have are shown. They are mainly based on personal commuications with the professors from the Department of Energy Sciences at the LTH and Compower AB.

The Mach number is the parameter that will give us a useful overview about the flow loading in the nozzle blades. It is important to know well the meaning of it. Mach number is defined as the ratio of the flow velocity to the local velocity of the sound. Therefore, this means that when we have a Mach number equal to 1, we get sonic velocity in the nozzle. It is normally represented in the vertical axis in the blade loading plots.

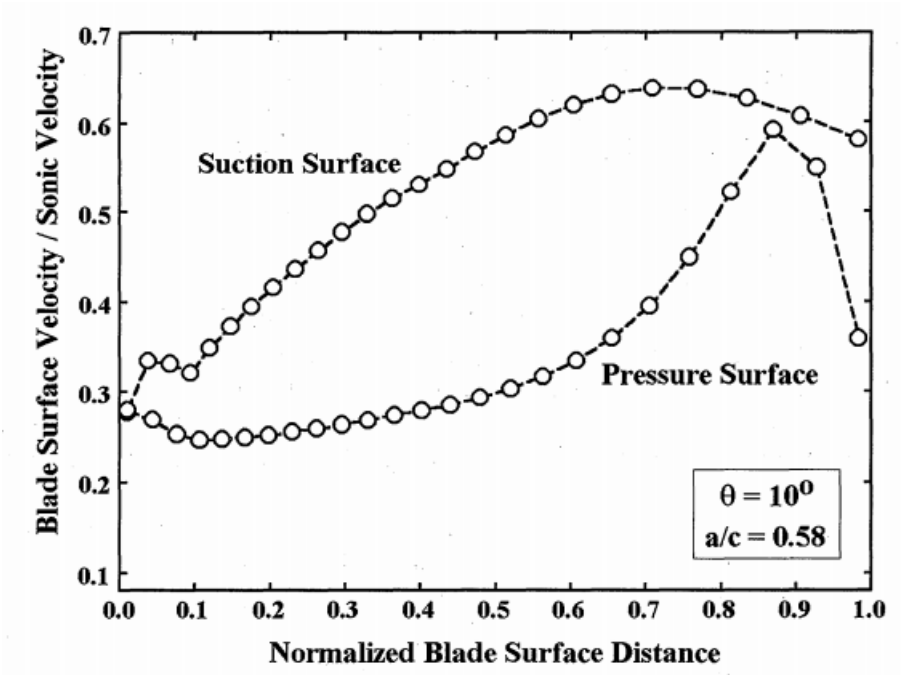

Figure 5.8: Blade loading plot for nozzle vanes. The normalized blade surface distance is obtained from the ratio axial distance/axial chord [3].

From the preliminary design, the maximum value of the Mach number was 0.65. This value could be apparently low, but considering Fig. 5.8 it is not. Therefore, there is a reason why no high Mach number values close to 1 are recommended. It is related to the losses. The higher the Mach number, the higher the pressure losses.

There is a correction factor K_M which depends directly on the Mach number squared, and it has a linear relationship with the pressure losses. This way, for instance having a Mach number of 1 will produce very higher losses than 0.6. The relation between K_M and M is shown on equation 5.1. Then in equation 5.2 the influence of the K_M factor to the profile loss coefficient is shown. The value of ε is defined as $\varepsilon = (90^o - \beta_1)/(90^o - \alpha_2)$. The rest of the presented parameters in the following equations are defined in the nomenclature of this document.

$$K_M = 1 + \left[1.65(M-0.6) + 240(M-0.06^2)\right](s/R_c)^{(3M-0.6)} \tag{5.1}$$

$$Y_p = K_{mod}K_{inc}K_M K_p K_{RE}\left\{\left[Y_{p1} + \varepsilon^2(Y_{p2} - Y_{p1})\right](5t_{max}/c)^{\varepsilon} - \Delta Y_{TE}\right\} \tag{5.2}$$

Also, it is important to keep a safety margin in the Mach number values. There are mainly two reasons for that:

- When getting M=1, the subsonic flow becomes transonic and then supersonic. The shock causes pressure losses, and even a small shock would result in losses.
- It is possible that in the three-dimensional flow analysis and in the real process the Mach number values go above 1 and this will cause shock waves, which would be harmful for the material as well as for the flow process itself.

Therefore, a good margin could be 0.1, what means that the maximum Mach number should be around 0.9. Also, the peak values below M=1 should take place at the blade dimensionless distance of 0.7. Then, the velocity should decrease very slowly. It is important to keep the deceleration process very controlled since a fast deceleration is always going to produce turbulent areas.

The Mach number setting process is going to be carried out through the modifications of the parameters that determine the shape of the airfoil. In Fig. 5.9 the clear difference between the camber and the chord line is shown. Having a blade camber angle of 0 degrees would mean to have a symmetric airfoil where the chord line and the camber line would match.

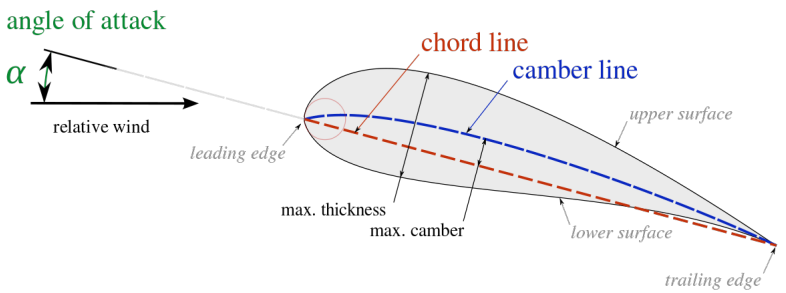

Figure 5.9: Airfoil drawing with chord and camber lines [15].

The parameters that have been adjusted in the process of the blade loading plot are as follows:

- **Discharge Pitch/Chord:** It is the non-dimensional throat at the end of the nozzle's passage. Pitch is the distance between two vanes, therefore it is the throat at the outlet of the vanes. The throat is the narrowest part of a blade

passage which also controls the mass flow rate through the passage. And the chord, as shown in Fig. 5.9 is the distance between the extremes of the leading and the trailing edge. Good values for this parameter are around 0.7 and the higher it is, the faster is the acceleration in the suction side of the blade. This parameter and the number of blades determine the inlet radius ratio.

- **Blade Camber Angle:** It is the angle between camber line and axial direction. It is refered to a simple airfoil shape. Its modifications can make possible to achieve supersonic flow, since it is easy to achieve M=1 just changing this parameter. It controls the blade inlet angle and the turning of the flow.

- **Distance to Maximum Camber/Chord:** The values between 0.25 and 0.75 will give a valid result, but the ones above 0.5 will achieve good distributions. It is useful to obtain a smooth variation of the blade camberline angle and blade passage area from inlet to discharge.

- **Distance to Maximum Thickness/Chord:** The maximum thickness as well as its location will also affect to the passage area distribution.

- **Maximum Thickness/Chord:** Note also that the thickness distribution has to be established based on mechanical considerations.

- **Inlet Thickness/Chord:** It is the characteristic parameter of the leading edge. A close value to 0.01 will be a good option, since based on the simulations, the higher it gets, the easier the pressure and suction surface lines intersect. And it is quite important to keep the suction side velocities higher than the pressure side all along the blade.

- **Discharge Thickness/Chord:** As well as the previous one, this is the characteristic for the trailing edge. Based on the performed simulations, an approximated value of 0.012 will give a good shape below the sonic velocity.

All the modifications of the previous parameters have been carried out in order to minimize the turbulences in the stator phase. However, it is almost impossible to achieve very uniform flow since for that it would be necessary to have a thickness of 0 at the trailing edge of the blade. This would mean to have a very weak blade and it would easily break under load. Therefore, the thickness at the trailing edge must be optimum, although it means to have a small drop for the flow that goes through the blade wall. The same happens in the impeller, the turbulences must be minimum since later in the diffuser it will increase. Note that in the diffuser the flow must have a slight deceleration in order to avoid turbulences.

Finally, bearing in mind the previous considerations, the main requirements that the blade loading plot of the nozzle vanes should meet have the following:

- The blade loading for subsonic blades should have a fast acceleration in the suction side. The flow should be accelerated all the way through and not at the outlet.

- In order to have a good behaviour of the flow at the vanes outlet, it is highly recommended to keep velocities at the trailing edge close to each other. Therefore, having high variations of the load Mach number value at suction and pressure sides must be completely avoided.

- The maximum value of the Mach number should not be higher than 0.9, since when doing CFD and in reality, the values can go above Mach 1 in case the blade loading plot has close values to 1. This would cause problems and shock waves. The presence of the boundary layer in the walls of the blade makes the throat narrower, what means that the real velocity is higher and also the Mach number. However, programs B2B2D and TDB2B take in consideration the presence of the boundary layer.

In Fig. 5.10 the result of the blade loading plot for the nozzle vanes of the microturbine is shown. As it can be seen the maximum Mach number is a bit lower than 0.9 and it is achieved in the dimensionless distance of 0.7. After that, at the outlet part the flow is slightly decelerated both surfaces but specially in the suction side.

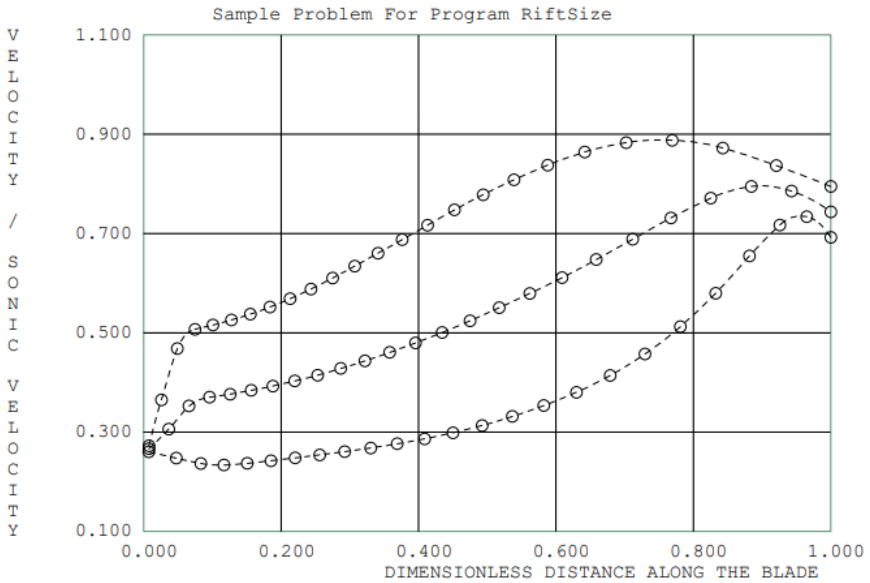

Figure 5.10: Blade loading plot for nozzle vanes obtained after the time-dependent blade to blade analysis. Picture taken from the output file of the TDB2B program from TurbAero

After running the programs RIFTNOZ, B2B2D and TDB2B many times sweeping each parameter to see how it affected to the blade loading plot, the best combination of them was achieved. It can be seen in Fig. 5.11.

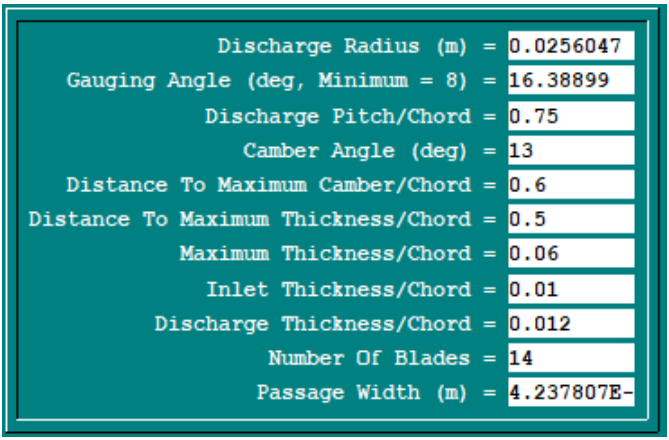

Figure 5.11: Final values of the geometric parameters of the nozzle used to get the final blade loading plot. Picture taken from blade geometry design data in RIFTNOZ.

5.4 Design of the impeller using GASPATH & BEZIER

In this section the procedure followed to obtain the geometry of the impeller is described. The starting point is the preliminary design obtained with RIFTSIZE. In fact, the input files for the packages GASPATH and BEZIER are obtained with RIFTSIZE. Also, it is important to note that both programs work on different files but when running GASPATH it needs the information from the BEZIER file in order to be run properly. Therefore, curve design is independent from the gas path design.

GASPATH designs hub and shroud contours and blades for turbomachinery components. It is the package that performs the simulations from which the the final results are obtained. They will be shown later. BEZIER develops curves to be used by GASPATH to construct the end-contours and blades. Commonly it is run before program GASPATH, but it can be accesed from GASPATH to modify the curves.

Program GASPATH can design two types of blades that can be very interesting for this work:

- **2D radial element blades:** Its camber line is composed of radial line elements. A blade angle distribution is created as a function of the axial coordinate and the radius. These angles are referred to the entire axial domain where blades exist.

- **General 3D blades:** The blade geometry is interpolated from hub to the shroud, using the camberlines for the hub, mean and shroud surfaces.

Blade thickness distribution

One of the main results that was longed and very important for the Compower AB was the blade thickness distribution of the impeller blades. The company developed a blade thickness distribution that was performed based on their experience. It has been used in their last designs and it is shown in Fig. 2.2.

Unfortunately, a complication arose and the blade thickness distribution could not be performed using GASPATH and BEZIER. A curve with the same distribution was created in BEZIER in order to match it then with the blade thickness distribution in GASPATH. The selected type of blade was a 2D radial element since it is not possible to do blade thickness distributions for a general 3D blade. However, when the blade thickness output plot was going to be obtained there was no connection between it and the distribution previously performed.

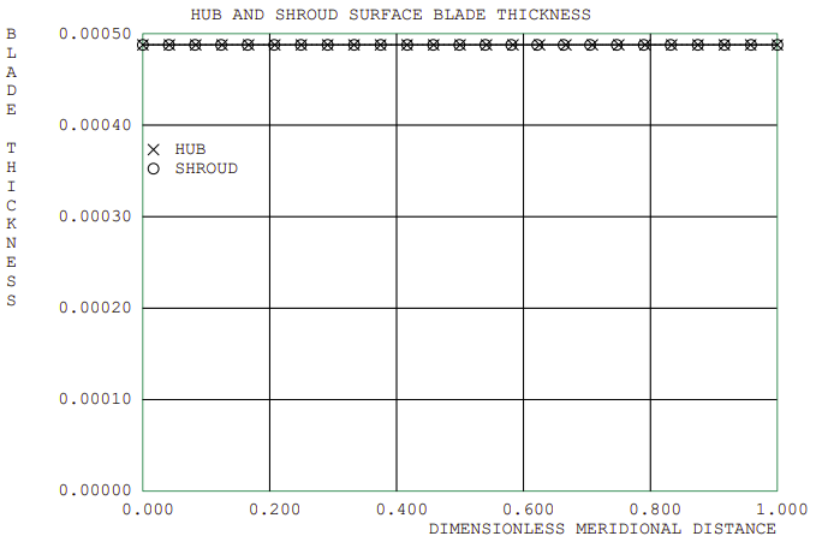

Figure 5.12: Constant blade thickness plot from GASPATH. The blade thickness in the vertical axis is measured in m and the dimensionless meridional distance is obtained from the ratio axial distance/axial chord.

Therefore the decided solution together with Compower AB and the Dpt. of Energy Sciences at LTH was to keep the blade thickness constant all along the blade in the gas path design process. The result is presented in Fig. 5.12.

Curve fit

In addition it was decided to fit the contour curves to Bézier distribution curves using the program BEZIER. These are parametric curves that are related to Bern-

stein polynomials. They are commonly used in computer graphics and similar fields. Bézier curves can also be combined to form a Bezier spline and Bézier surfaces in higher dimensions.

The Bernstein-Bezier polynomial is a recommendable method for generating curves using a series of reference points. A smooth curve is always generated, and it will have the next characteristics:

- Have the same slope at the end points as a line connecting the end reference points and their adjacent reference points.
- Pass through the start and end reference points.
- Respond to changes in reference point coordinates by moving less than 1/3 the reference point change, in the same direction.
- Have end-point curvatures set by the first and last 3 reference points.

Table 5.1 shows the available curves in BEZIER program that are available to be used in GASPATH after fitting the hub and shroud contours curves in Bernstein-Bezier curves. Likewise, Table 5.2 shows the selection of suitable curves in GASPATH.

Table 5.1: List of existing curves in program BEZIER after fitting the hub and shroud contour curves with Bezier curves.

CAPTIONS OF EXISTING CURVES
1) Circular-Arc Hub Contour (RIFTSIZE)
2) Shroud Contour Coordinates (RIFTSIZE)
3) Radial Element Blade Angles (RIFTSIZE)
4) [Bezier Fit] Circular-Arc Hub Contour (RIFTSIZE)
5) [Bezier Fit] Shroud Contour Coordinates (RIFTSIZE

Table 5.2: List of curves match in program GASPATH. The hub and shroud contour curves are assigned to the Bezier fit ones.

CURVE TYPE	*CURVE TYPE SELECTION*
Hub Contour	[Bezier Fit] Circular-Arc Hub Contour (RIFTSIZE)
Shroud Contour	[Bezier Fit] Shroud Contour Coordinates (RIFTSIZE)
2D Blade Thickness Distribution	Constant Thickness/Leading Edge Taper
2D Blade Angle Distribution	Radial Element Blade Angles (RIFTSIZE)

Afterwards, once the curves fit is performed, the frontal and side views of the impeller blades can be obtained. The frontal view of the blades is shown in Fig. 5.13 while the side view of the blades is shown in Fig. 5.14. In the side view of the blade the quasi-normals that have been used in the simulations can be seen. 29 quasi-normals have been used, the blade leading edge is located in the quasi-normal number 3 and the blade trailing edge is located in the quasi-normal number 27. When deciding the number of quasi-normals it is also possible to select the direction of rotation. Counterclockwise direction was selected.

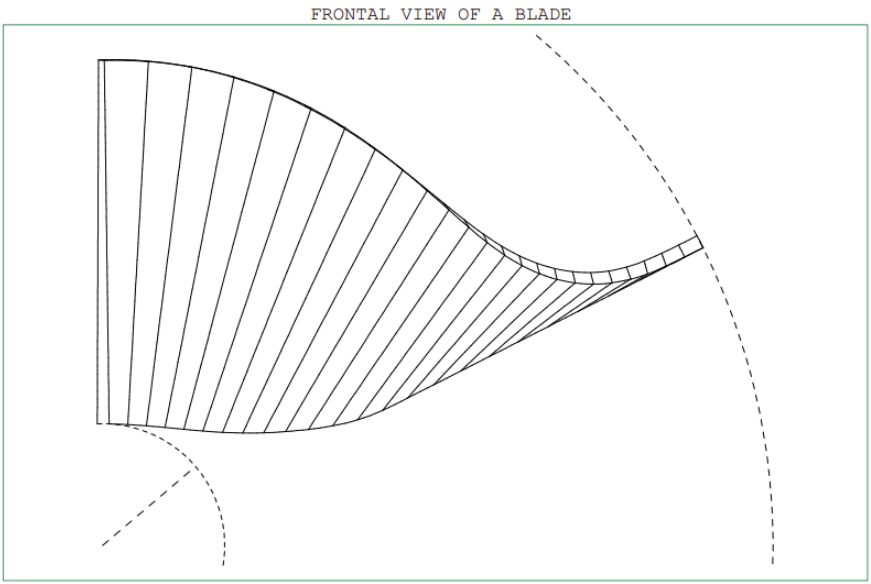

Figure 5.13: Frontal view of the impeller blades from GASPATH.

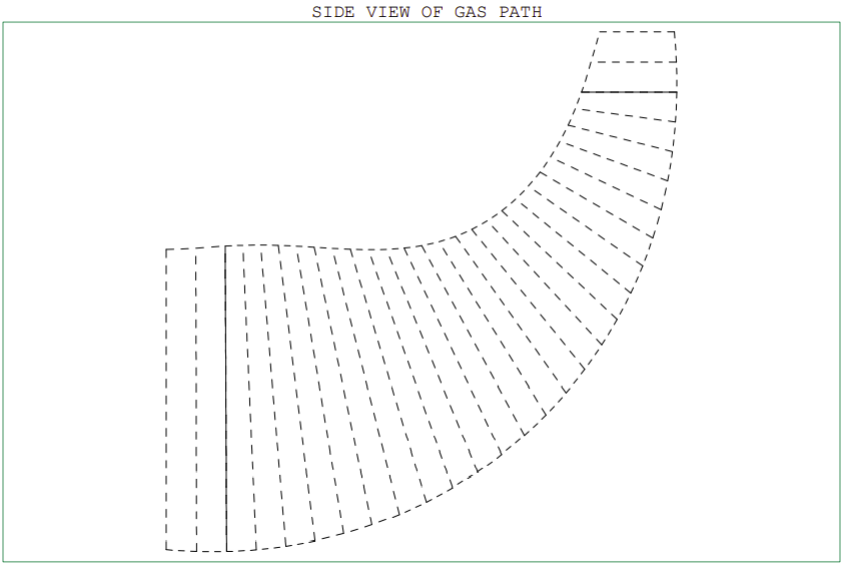

Figure 5.14: Side view of the impeller blades from GASPATH. 29 quasi-normals have been used to do the simulations.

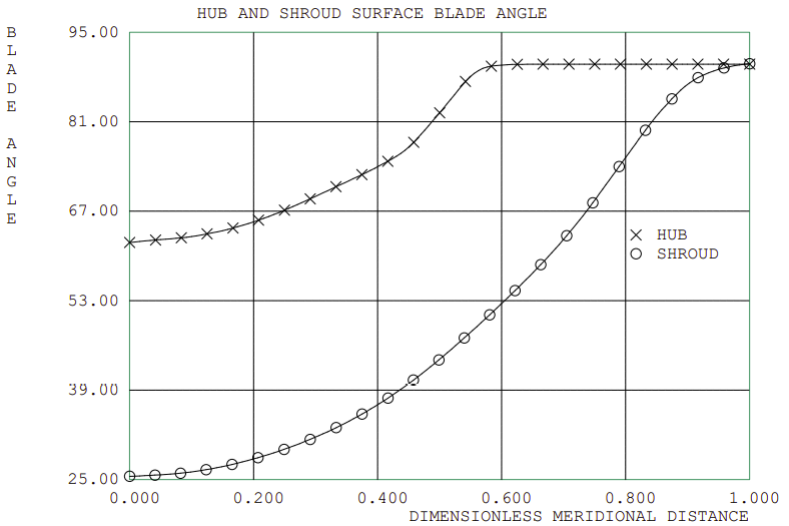

Figure 5.15: Surface blade angles in the hub and shroud from GASPATH.

Figure 5.15 shows the blade angle distribution all along the hub and shroud surfaces. As seen, there is a difference between blade angle values in hub and shroud, but then they finally get same values at the outlet of the impeller, which will make the flow exit in a straightforward way. Obtaining these similar values is recommended in order to avoid turbulence and sudden pressure drops.

6

Concluding remarks and future work

6.1 Conclusion

The aim of this master thesis was to perform the aerodynamic design of a radial-inflow microturbine for a combined heat and power generation unit. This has been mainly conducted with the tool TurbAero, which consists on several packages for the design of different turbomachine components. This project has been carried out at Compower AB in cooperation with the Dept. of Energy Sciences at LTH.

The result of this master thesis is an aerodynamic design of a radial-inflow microturbine. The correct management of the simulations, each parameter and the calculations have been the core of this work. The dimensional analysis and the study of the equations and parameters involved have been carried out before the design and they have been really important in order to have a good understanding of all the material. Likewise, the applications and the state of the art explained in the introduction chapter have been useful to understand some of the research methods in microturbine design and the actual use of microturbines as well. Moreover, in the introduction it has been shown that microturbines are a flexible and suitable solution for many different applications, which has been a motivation for this work.

TurbAero has proven to be a powerful tool for turbine design. It has been possible to obtain both graphical and numerical results at any moment which has been very useful in order to do modifications and comparisons in an easy way. However two limitations have been discovered. The software could not be used for designing the blade thickness distribution along the impeller blades and the results of the preliminary nozzle design were not satisfactory. However these difficulties were overcome.

In conclusion, after the preliminary design of various components of radial-inflow microturbine, the detailed design for the nozzle vanes and the impeller blades were performed in order to get the correct Mach number and loading distributions.

6.2 Future work

The results of this work provide the basis to start the next steps in the project of Compower AB. There are two main steps that have to be carried out before the manufacturing phase. They are the geometry generation and the three dimensional flow analysis.

For the first step, that is the geometry generation some more aerodynamic analysis has to be done. It is important to know that during this work the geometry of the impeller and the nozzle vanes was created with a 3D CAD generator several times in order to check the set up. They can be seen at the Appendix A3.

Once the geometry generation is finished, the three dimensional flow analysis has to be performed. It will be very useful to check that there are not turbulent areas all along the flow path. This will be done with a CFD software. In addition, structural and stress analysis in the microturbine components is likely to be necessary. There are some programs that are capable of performing both the flow analysis and the stress analysis, as well as additional analysis.

Finally, the microturbine will be manufactured and may be tested on a test bench of the Compower AB either in Malmö or in Stockholm. Afterwards, it will be launched to the market and it will be commercialized.

For the future work of this project, it is good to know some of the incidents that have arisen during the development of the microturbine design. The most representative ones are explained below.

Nozzle vanes

After performing the preliminary design, it was decided to keep the nozzle vanes geometry proposed by RIFTSIZE. Note that the component geometry of the microturbine is obtained from the software in an output file that contains the coordinates. In order to check the result given by the program, it was decided to draw in a 3D CAD generator program the nozzle vanes geometry.

Once the profile of the nozzle blades was drawn, the result was a very straight and flat shape, which at first glance, is not very recommendable. This shape of the nozzle vanes is not the most suitable to obtain good Mach number values. In fact, the Mach number at the outlet of the vanes was apparently low. Therefore, the solution consisted on performing all the necessary simulations to obtain the best loading plot. As explained in the previous chapter, a good shape of the blade loading plot means to have a good velocity distribution all along the vanes and it is also highly related to the Mach number value and to the creation of turbulence at the exit of the nozzle.

Blade thickness distribution

The blade thickness distribution has been one of the main issues with more complications. The original idea was to perform the blade thickness distribution based on the one provided by Compower AB shown in Fig. 2.2 with the packages GASPATH

and BEZIER. In order to do that, two types of blades were used: 3D general blades and 2D radial blades. In neither case, there was no relationship between the results in GASPATH and the thickness distribution performed in BEZIER.

Therefore it was decided to keep a constant thickness during the impeller design in both GASPATH and BEZIER softwares, in order to perform the corresponding thickness distribution in possible next steps of 3D CAD generation.

7

References

[1] Capstone Turbines. *Products. C65*. URL: https://www.capstoneturbine.com/products/c65. (accessed: 13.04.2021).

[2] N. Baines. *Turbine Design and Analysis*. Digital edition, 2019.

[3] R. H. Aungier. *Turbine aerodynamics: axial-flow and radial-inflow turbinedesign and analysis*. New York, Asme Press, 2006.

[4] Yu. Ya. Fershalov et. al. "Microturbine with new design of nozzles". *ScienceDirect* (2018). URL: https://www.sciencedirect.com/science/article/abs/pii/S0360544218309976.

[5] D. Ibrahimov, A. Mochalov. "Research data of microturbine nozzles with outlet angles under 9 degree". *ScienceDirect* (2017). URL: https://www.sciencedirect.com/science/article/pii/S1877705817351895.

[6] A. Yu. Fershalov et. al. "Principles of designing gas microturbine stages". *ScienceDirect* (2020). URL: https://www.sciencedirect.com/science/article/pii/S0360544220325950.

[7] Mark R. Madler. "Turbine firm rebrands, experiments with hydrogen fuel." *San Fernando Valley Business Journal* (2021). URL: https://d1io3yog0oux5.cloudfront.net/_58354dc32461a80608be6ec57fef81c1/capstonegreenenergy/db/198/9658/pdf_article/SFVBJ_Digital_Edition_10May21_.pdf.

[8] Eva Konecná and Sin Yong Teng. "New insights into the potential of the gas microturbine in microgrids and industrial applications". *ScienceDirect* (2020). URL: https://www.sciencedirect.com/science/article/pii/S1364032120303695.

[9] Capstone Turbines. "Felsineo La Mortadella. Food Manufacturer" (2014). URL: https://d1io3yog0oux5.cloudfront.net/_da3c285f77c1a64176bee329b5f6467a/capstonegreenenergy/db/185/6491/pdf/CS_CAP438_Felsineo.pdf.

[10] Capstone Turbines. "Utility Software Company" (2017). URL: https://d1io3yog0oux5.cloudfront.net/_da3c285f77c1a64176bee329b5f6467a/capstonegreenenergy/db/185/7386/pdf/CS_CAP452_UtilitySoftware.pdf.

[11] V. Aa. *Apuntes de Mecánica de Fluidos*. ETSII. Polytechnic University of Valencia, 2017.

[12] S. Dixon and C. Hall. *Fluid Mechanics and Thermodynamics of Turbomachinery*. Butterworth-Heinemann, 2014.

[13] O. Balje. *Turbomachines: A Guide to Design Selection and Theory*. Sons Inc., 1981.

[14] Ronald H. Aungier. "TurbAero software user's guide" (2011). URL: https://www.turbo-aero.com/turbaero.

[15] Cleynen, O. *Airfoil nomenclature*. URL: https://en.wikipedia.org/wiki/Airfoil. (accessed: 15.05.2021).

A

Appendix

A.1 Cross sectional drawings from TurbAero

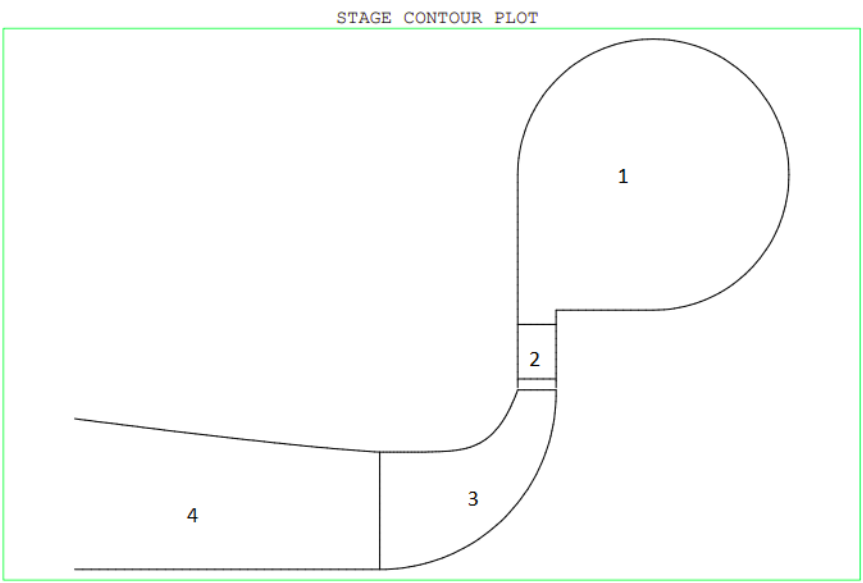

Figure A.1: Stage half cross section from the output file of RIFTSIZE.

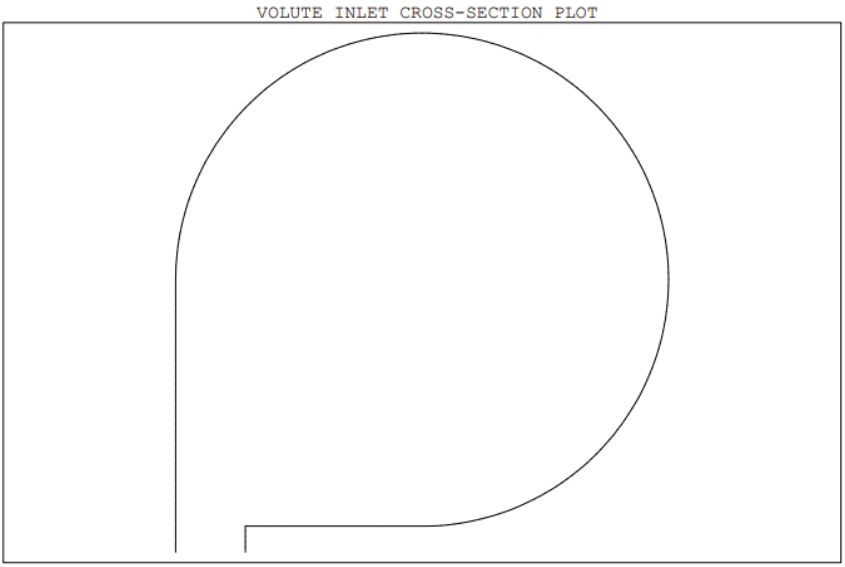

Figure A.2: Cross section of the volute from the output file of RIFTSIZE.

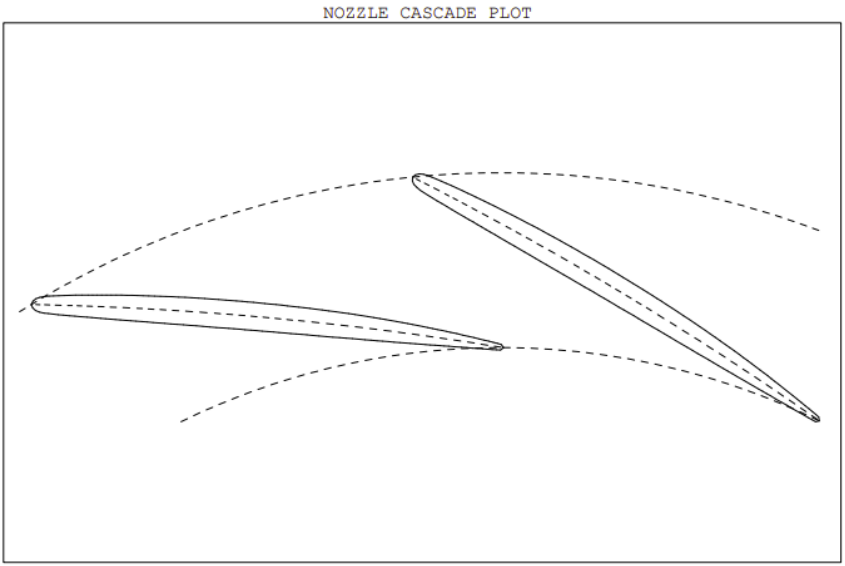

Figure A.3: Nozzle cascade plot from the output file of RIFTSIZE.

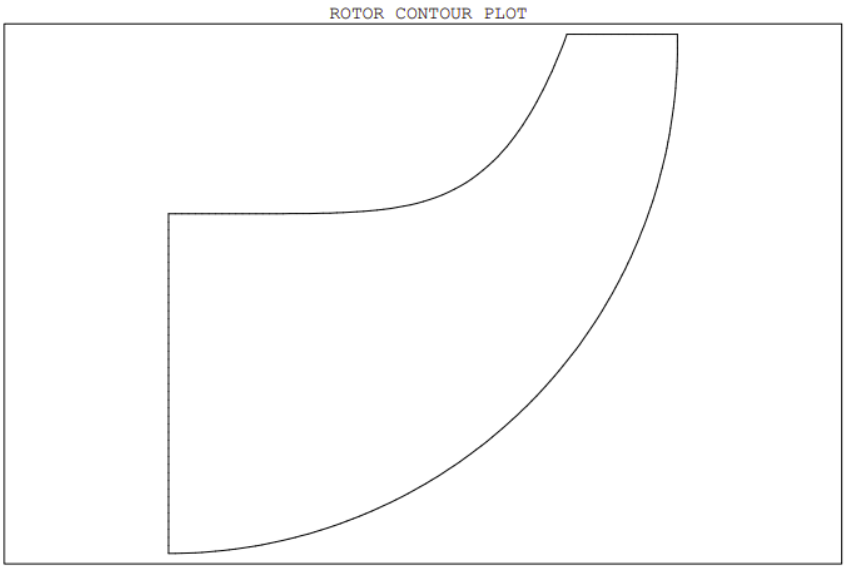

Figure A.4: Rotor contour plot from the output file of RIFTSIZE.

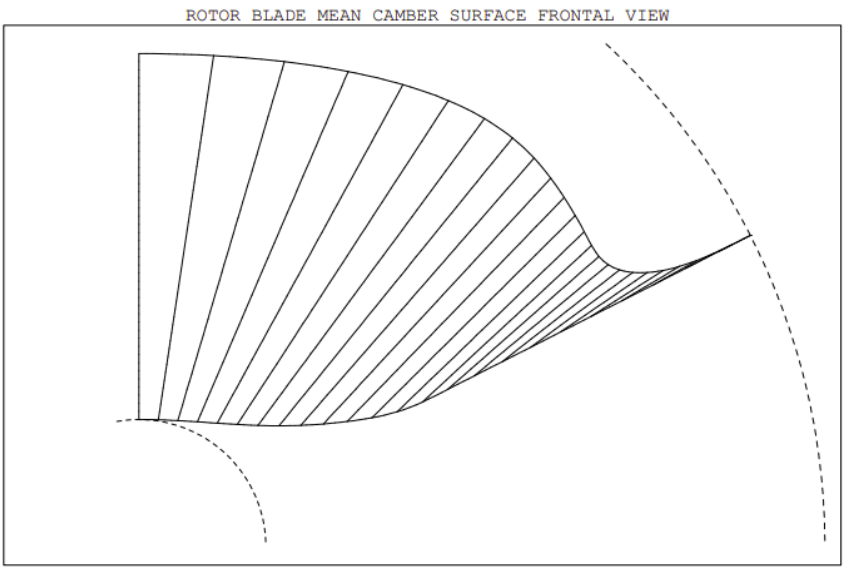

Figure A.5: Rotor blade mean camber surface frontal view from the output file of RIFTSIZE.

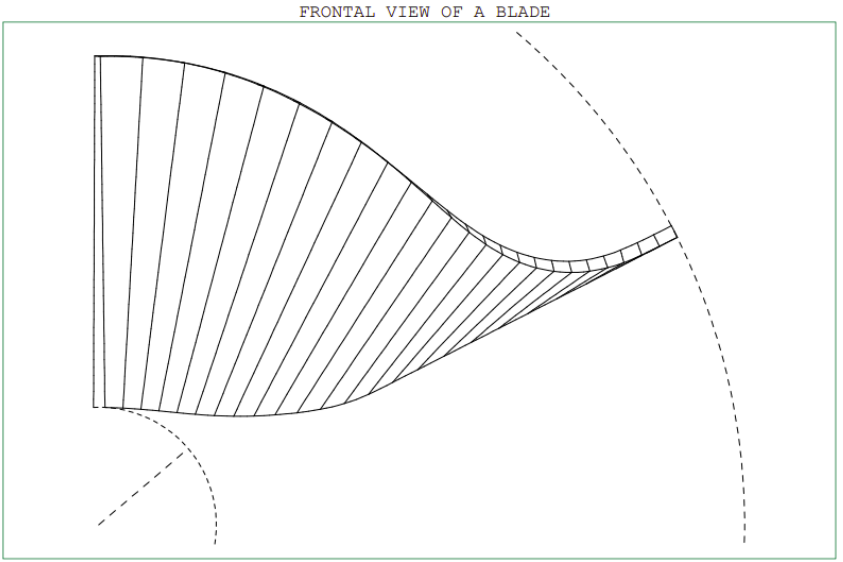

Figure A.6: Rotor blade frontal view from the output file of GASPATH.

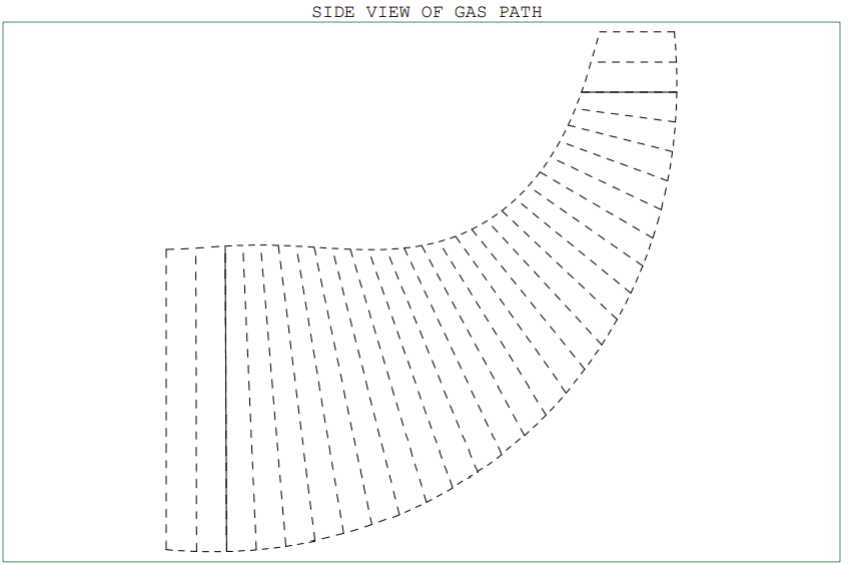

Figure A.7: Side view of the impeller blades from GASPATH. 29 quasi normals have been used to run the simulations. The leading edge is located in quasinormal number 3, and the trailing edge is located in number 27.

A.2 Blade loading plots in nozzle vanes

Here some of the blade loading plot that have been obtained from the simulations and sweping the parameters shown in Fig. 5.11 are shown. The nomenclature used in order to identify which parameter values have been used in each simulation is as follows: Discharge Pitch/Chord - Camber Angle - Distance to maximum Camber/Chord - Distance to Maximum Thickness/Chord - Maximum Thickness/Chord - Inlet Thickness/Chord - Discharge Thickness/Chord. The number of blades run has always been 14, since it was really important for Compower AB. The discharge radius, the gauging angle and the passage width have been kept as default values suggested by the program and are also shown in Fig. 5.11.

In order to understand and see how the variation of any parameter affects to the blade loading plot, the values are mentioned in the caption of each picture.

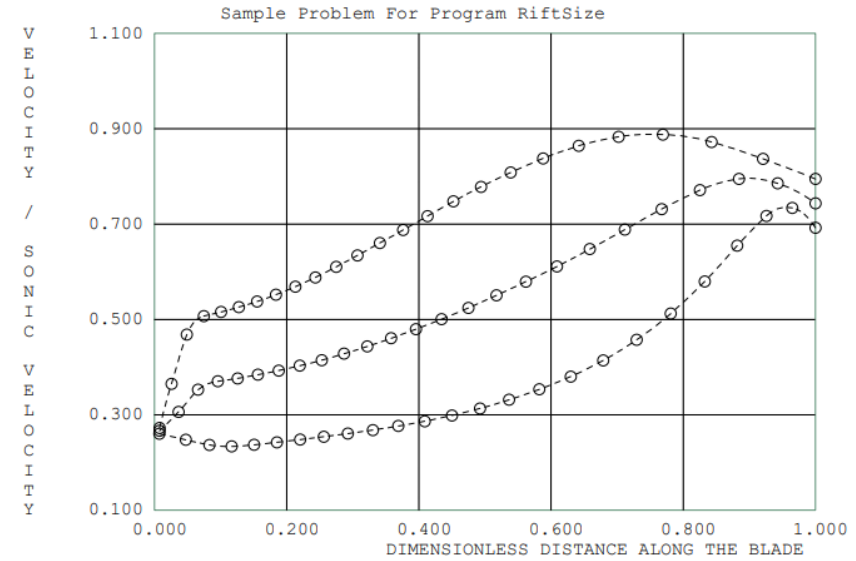

Figure A.8: Blade loading plot for nozzle vanes. This was the selected one for the final design. This is a screenshot from the output file. The values of the parameters: 0.75-13-0.6-0.5-0.06-0.01-0.012.

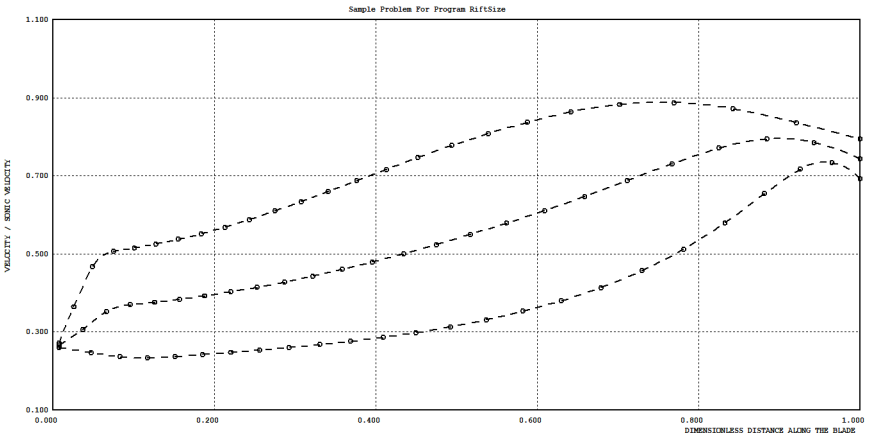

Figure A.9: Blade loading plot for nozzle vanes. This was the selected one for the final design. This is a screenshot from the program, so it will be easier to compare it with the following ones. The values of the parameters: 0.75-13-0.6-0.5-0.06-0.01-0.012.

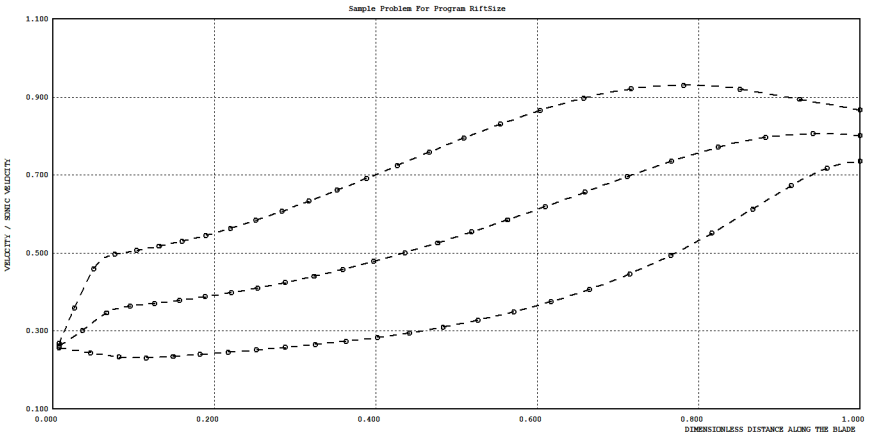

Figure A.10: Blade loading plot for nozzle vanes. The values of the parameters: 0.75-13-0.6-0.5-0.06-0.01-0.024.

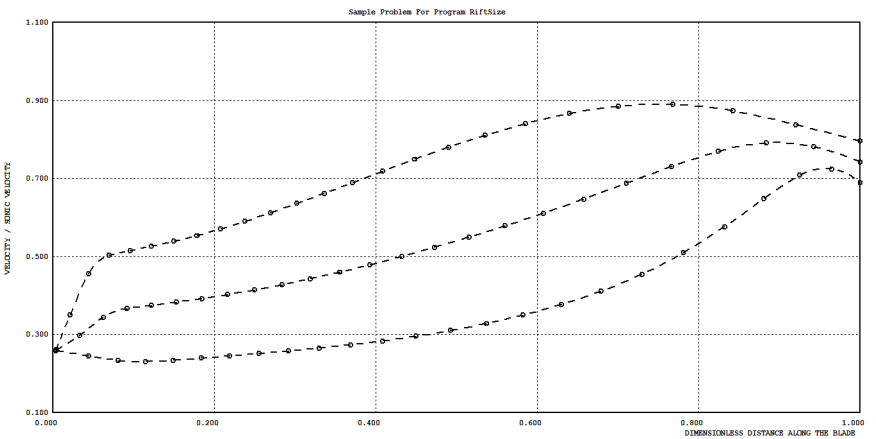

Figure A.11: Blade loading plot for nozzle vanes. The values of the parameters: 0.75-13-0.60-0.50-0.06-0.005-0.012.

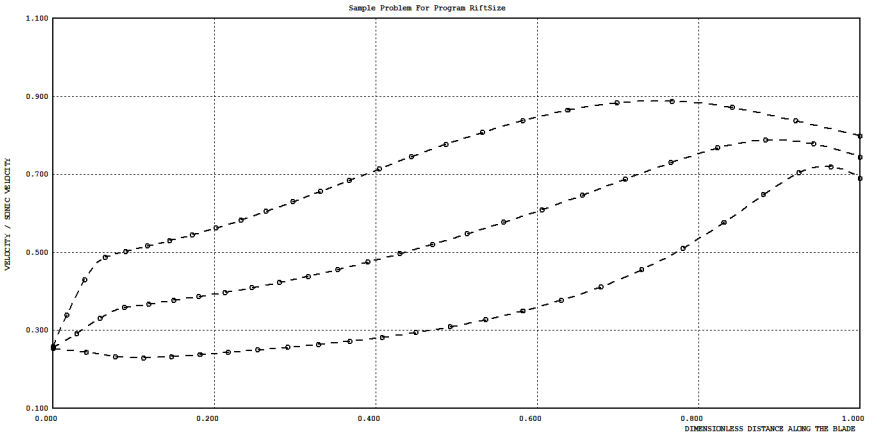

Figure A.12: Blade loading plot for nozzle vanes. The values of the parameters: 0.75-13-0.60-0.50-0.06-0.0001-0.012.

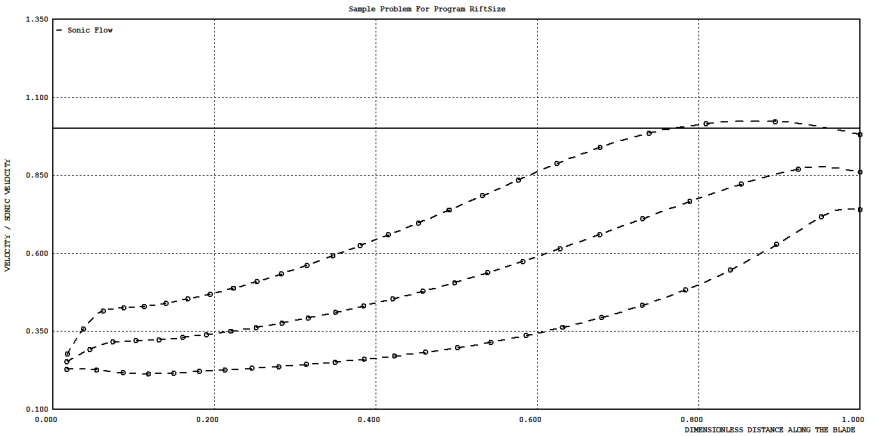

Figure A.13: Blade loading plot for nozzle vanes. The values of the parameters: 0.7-7-0.58-0.4-0.06-0.025-0.012.

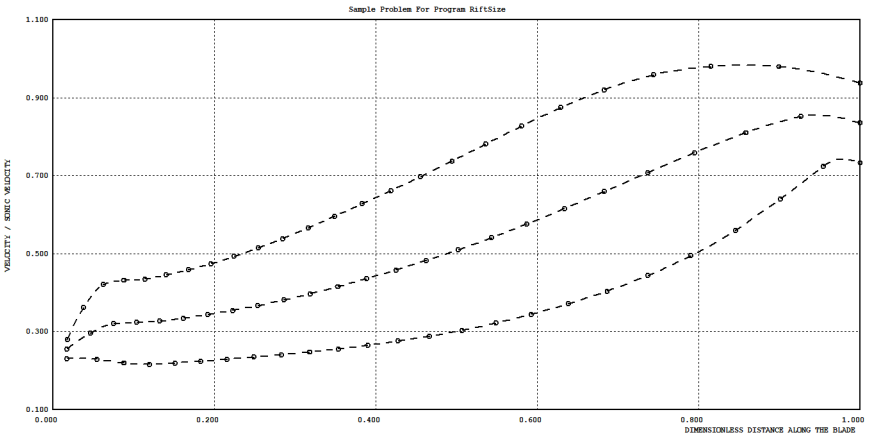

Figure A.14: Blade loading plot for nozzle vanes. The values of the parameters: 0.7-8-0.58-0.4-0.06-0.025-0.012.

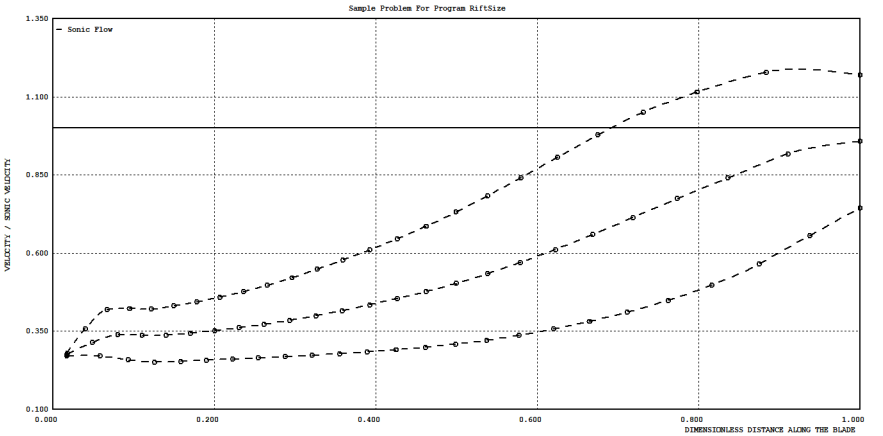

Figure A.15: Blade loading plot for nozzle vanes. The values of the parameters: 0.7-10-0.40-0.40-0.06-0.025-0.012.

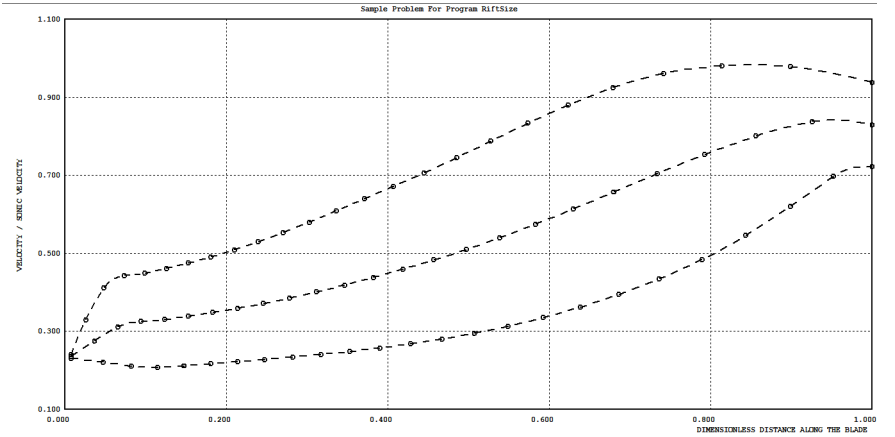

Figure A.16: Blade loading plot for nozzle vanes. The values of the parameters: 0.7-10-0.58-0.4-0.06-0.01-0.012.

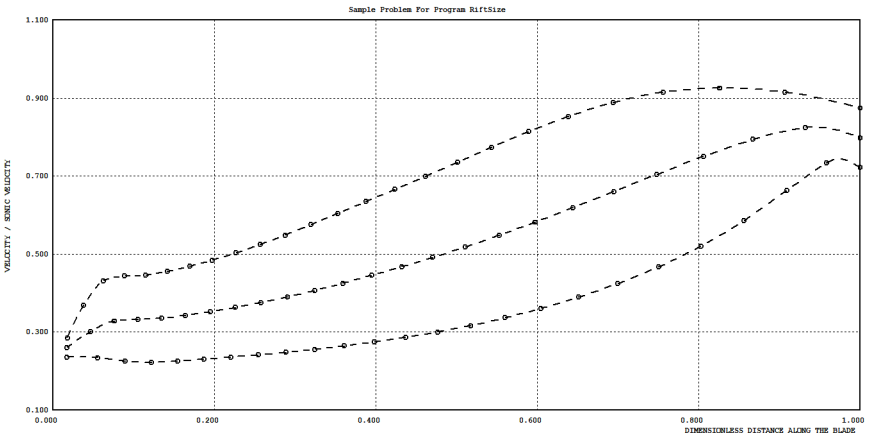

Figure A.17: Blade loading plot for nozzle vanes. The values of the parameters: 0.7-10-0.58-0.4-0.06-0.025-0.012.

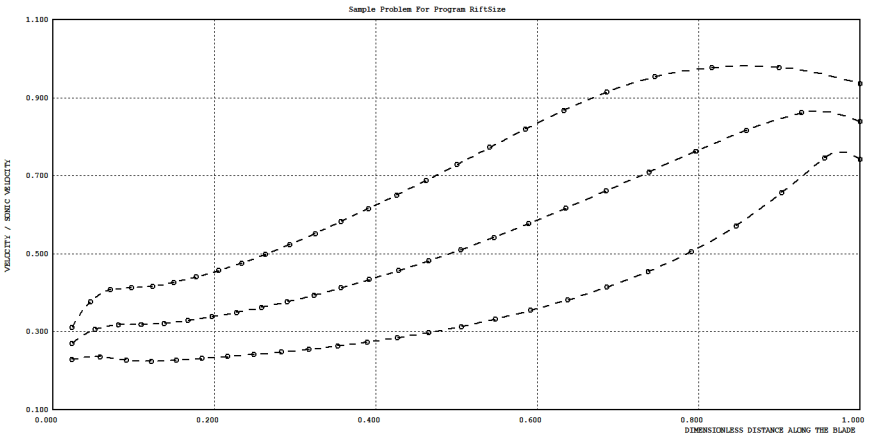

Figure A.18: Blade loading plot for nozzle vanes. The values of the parameters: 0.7-10-0.58-0.4-0.06-0.035-0.012.

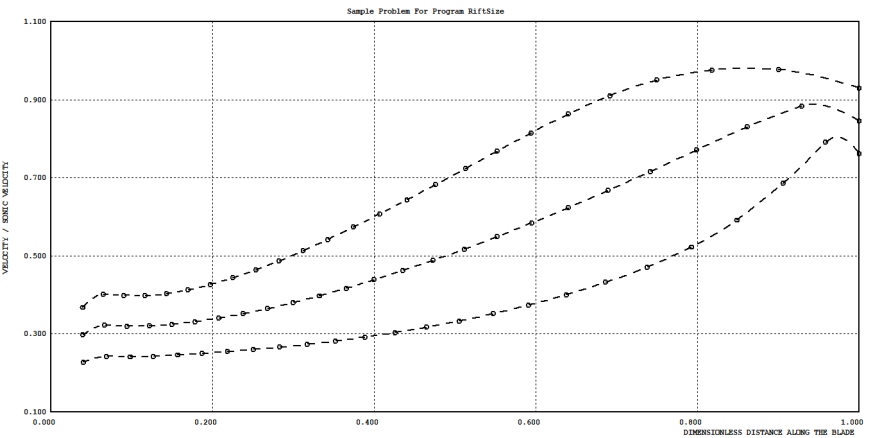

Figure A.19: Blade loading plot for nozzle vanes. The values of the parameters: 0.7-10-0.58-0.4-0.06-0.055-0.012.

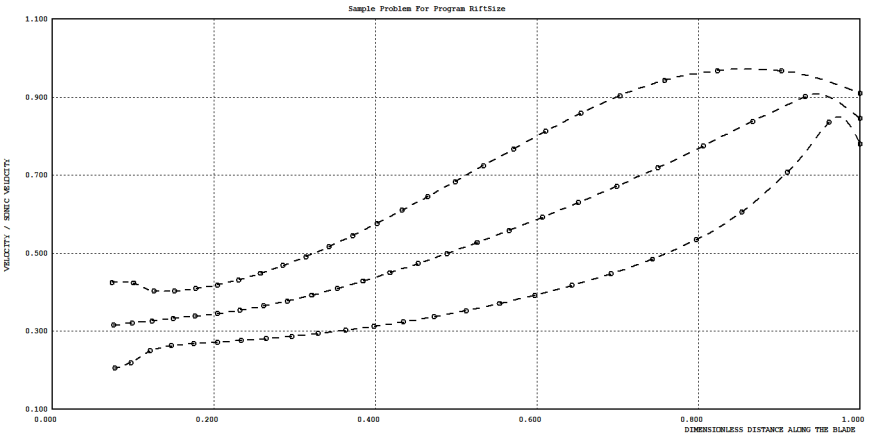

Figure A.20: Blade loading plot for nozzle vanes. The values of the parameters: 0.7-10-0.58-0.4-0.06-0.075-0.01

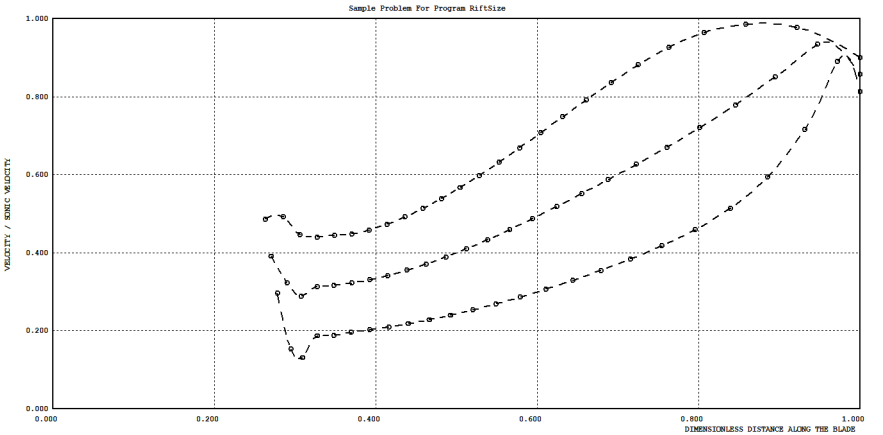

Figure A.21: Blade loading plot for nozzle vanes. The values of the parameters: 0.7-10-0.58-0.4-0.06-0.100-0.012.

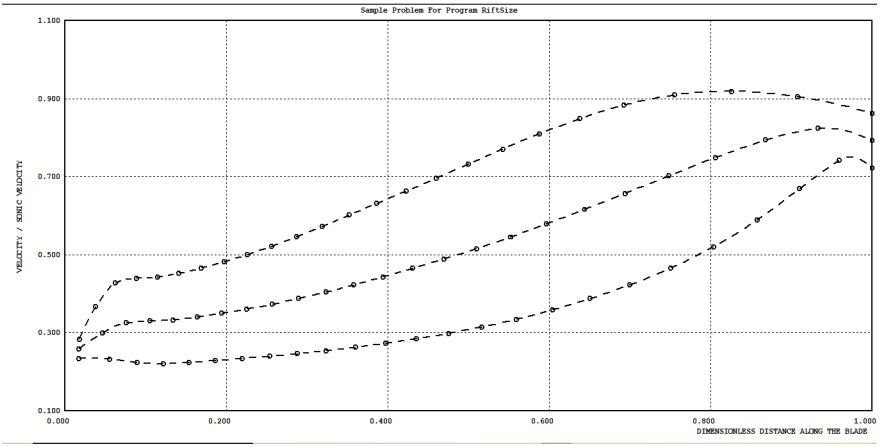

Figure A.22: Blade loading plot for nozzle vanes. The values of the parameters: 0.7-10-0.59-0.4-0.06-0.025-0.012.

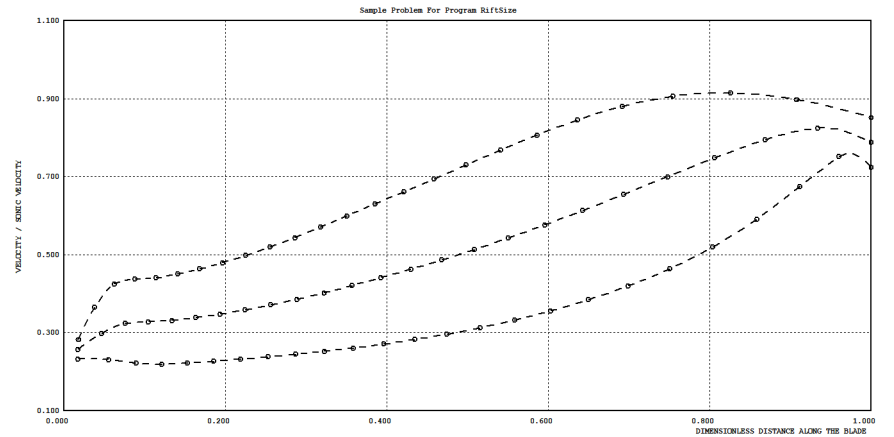

Figure A.23: Blade loading plot for nozzle vanes. The values of the parameters: 0.7-10-0.60-0.4-0.06-0.025-0.012.

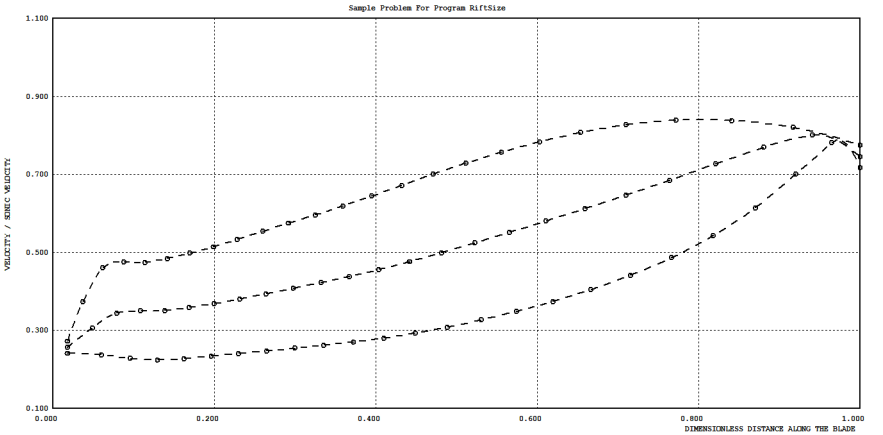

Figure A.24: Blade loading plot for nozzle vanes. The values of the parameters: 0.7-13-0.60-0.30-0.06-0.025-0.012.

A.3 Geometry generation tests

The following pictures present the tests of the geometry generation that have been performed throughout the aerodynamic design in order to check the appearance of the resulting 3D model.

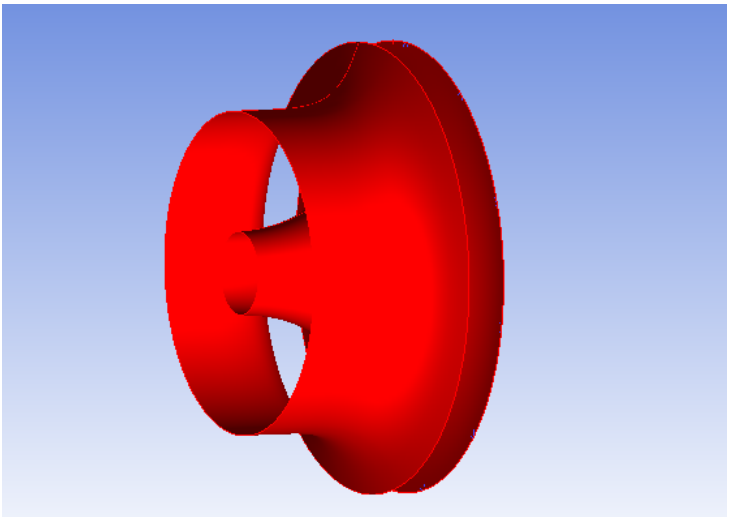

Figure A.25: 3D geometry generation test of the hub and the shroud of the impeller.

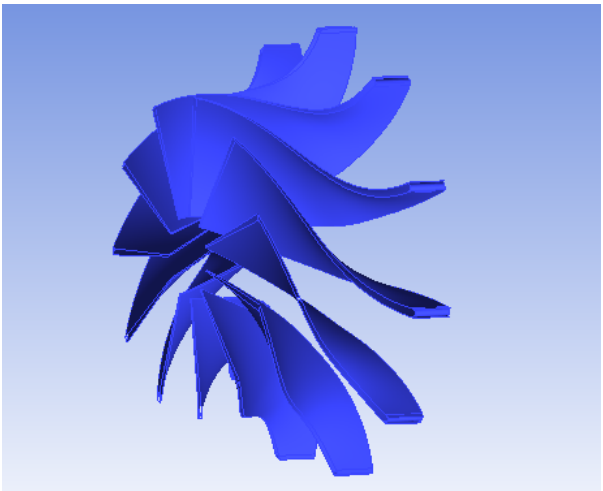

Figure A.26: 3D geometry generation test of the impeller blades.

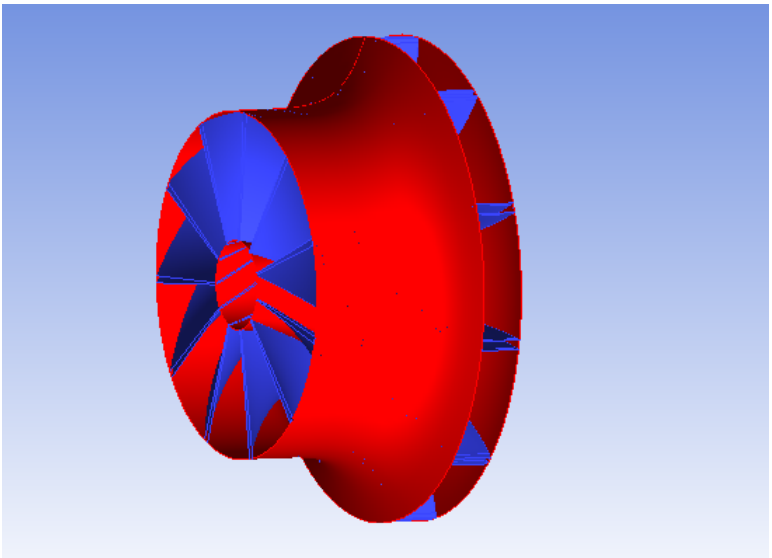

Figure A.27: 3D geometry generation test of the impeller blades and casing.

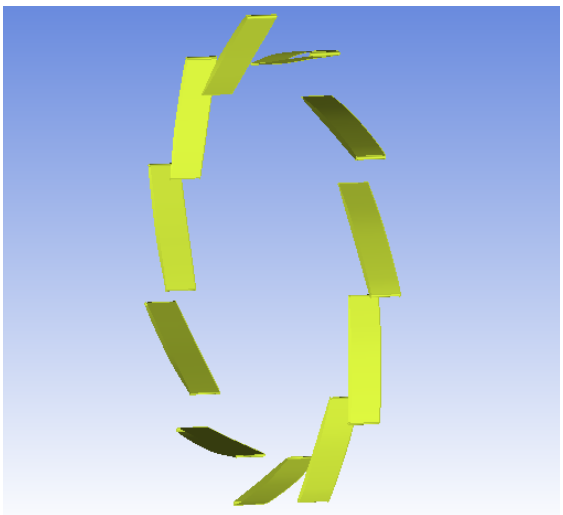

Figure A.28: 3D geometry generation test of the nozzle vanes based on the results from preliminary design.

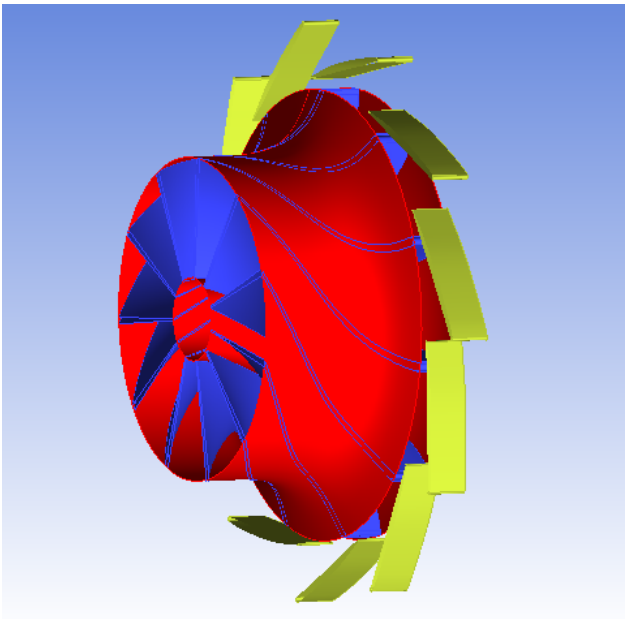

Figure A.29: 3D geometry generation test of the impeller and the nozzle vanes.